

1 **Modeling long-term fire regimes of southern California shrublands**

2
3 *(Suggested running head: “Modeling fire regimes with HFire”)*

4
5 **Seth H. Peterson^a, Max A. Moritz^b, Marco E. Morais^c, Philip E. Dennison^d, and Jean M.**
6 **Carlson^e**

7
8
9 ^a*Department of Geography, UC Santa Barbara, CA 93106, USA*

10 ^b*Center for Fire Research & Outreach, Department of Environmental Science, Policy, & Management,*
11 *UC Berkeley, CA 94720, USA*

12 ^c*The Aerospace Corporation, 2350 E. El Segundo Blvd, El Segundo, CA 90245, USA*

13 ^d*Center for Natural and Technological Hazards, Department of Geography, University of Utah, Salt Lake City, UT*
14 *84112, USA*

15 ^e*Department of Physics, UC Santa Barbara, CA 93106, USA*

16
17
18
19 Corresponding author email: seth@geog.ucsb.edu, phone: 805-893-4434

22 **Abstract**

23 This paper explores the environmental factors that drive the southern California chaparral fire
24 regime. Specifically, we examined the response of three fire regime metrics (fire size
25 distributions, fire return interval maps, cumulative total area burned) to variations in the number
26 of ignitions, the spatial pattern of ignitions, the number of Santa Ana wind events, and live fuel
27 moisture, using the HFire fire spread model. HFire is computationally efficient and capable of
28 simulating the spatiotemporal progression of individual fires on a landscape and aggregating
29 results for fully resolved individual fires over hundreds or thousands of years to predict long-
30 term fire regimes. A quantitative understanding of the long term drivers of a fire regime is of use
31 in fire management and policy.

32

33 **50 Word Summary**

34 This paper uses a new fire spread model, HFire, to examine the drivers of the fire regime in
35 southern California shrublands, namely: the number of ignitions per year, the spatial pattern of
36 ignitions, the number of Santa Ana wind events per year, and live fuel moisture.

37 **Introduction**

38 The fire regime of a landscape integrates the spatiotemporal pattern of ignitions, fuels, weather,
39 and topography, and describes the size, spatial pattern, and return interval of fires (Davis and
40 Michaelsen 1995). The current fire regime of southern California shrublands extends over a
41 broad range of fire sizes from numerous small fires to relatively few large, intense, stand
42 replacing fires, at a 20 to more than 100 year recurrence interval (Davis and Michaelsen 1995;
43 Moritz 1997; Keeley 2000; Moritz *et al.* 2005). Past fire regimes in chaparral may have been
44 quite similar, with total area burned also dominated by large fires (Mensing *et al.* 1999; Keeley
45 and Fotheringham 2003). This distribution of fire sizes is common to other fire prone ecosystems
46 as well (Moritz *et al.* 2005).

47 Fire regimes are dynamic, varying in response to changes in ignition frequency,
48 vegetation, and climate. In the future, climate change will likely have an effect on fuel quality
49 and amount, while increases in population in the wildland urban interface (WUI) will likely lead
50 to increased number of ignitions and changes in ignition locales (Field *et al.* 1999; Keeley and
51 Fotheringham 2003; Syphard *et al.* 2007; Moritz and Stephens 2008). A quantitative
52 understanding of fire regime drivers will aid in understanding future fire regimes resulting from
53 climate change and the expansion of the WUI.

54 In this paper we evaluate the sensitivity of three fire regime characteristics (size
55 distributions, maps of fire return intervals (FRIs), and cumulative total area burned) to the
56 number and spatial pattern of ignitions; the frequency of extreme, Santa Ana wind conditions;
57 and live fuel moisture (LFM) using HFire, a landscape fire succession model (LFSM). HFire
58 uses a mechanistic approach to modeling fire spread, using the full Rothermel (1972) equations.
59 It is capable of modeling both individual fires and long-term fire regimes in southern California

60 chaparral shrubland landscapes (Peterson *et al.* 2009). The predictions of fire perimeters in HFire
61 have been validated in baseline comparisons to FARSITE (Finney 1998) and hourly progressions
62 of individual, southern California fires (Peterson *et al.* 2009). Modeled fire size distributions
63 from the initial version of HFire have been shown to agree with fire size distributions for the Los
64 Padres National Forest fire data between 1911 and 1995 (Moritz *et al.* 2005).

65 The southern California shrubland fire regime and HFire together provide a unique
66 evaluation study for comparing actual data with model results over broad spatial and temporal
67 scales. The relatively short southern California FRI provides an extended historical record of
68 observations, and the computational efficiency of HFire enables quantitative evaluation of which
69 physical parameters (ignitions, wind, LFM) are most important for determining the fire regime.

70

71 **Background**

72 *Landscape fire successional modeling*

73 Fire modeling is a viable approach for increasing our knowledge of fire regime dynamics under a
74 suite of conditions (Davis and Michaelsen 1995; Keeley and Fotheringham 2003; Keane *et al.*
75 2004; Franklin *et al.* 2001; Cary *et al.* 2006). Long-term simulation of fire and vegetation
76 response has been used to examine variation in existing landscape patterns (Venevsky *et al.*
77 2002), fire effects on vegetation dynamics (Haydon *et al.* 2000; Franklin *et al.* 2001), and
78 scenarios of management activities (Haydon *et al.* 2000; Miller and Urban 2000), and climate
79 change (Davis and Michaelsen 1995; Cary and Banks 1999).

80 Keane *et al.* (2004) categorized the 44 most well known LFSMs based on their approach
81 to modeling four main processes: (1) vegetation succession, (2) fire ignition, (3) fire spread, and
82 (4) fire effects. They found that for three of the processes the models varied in degrees of

83 stochasticity, complexity, and mechanism. However, a majority (36) of the models used a simple
84 probabilistic approach to modeling fire spread or final fire perimeters. Only eight of the models
85 used a mechanistic approach (Rothermel 1972; Finney 1998) to simulate fire spread in an
86 incrementally expanding manner.

87 Historically, mechanistic fire spread models have been considered too complex, computer
88 intensive, and/or the data requirements too vast for use in long-term fire regime simulations
89 (Hargrove *et al.* 2000; Venevsky *et al.* 2002), though their use would be preferable to empirical
90 or stochastic approaches if they could be implemented (Keane and Finney 2003). Of the eight
91 mechanistic models in the Keane *et al.* (2004) study, only Cary and Banks (1999) and Perera *et*
92 *al.* (2008) simulated fire spread at hourly time steps with the same rigor as single event fire
93 spread models (e.g., Finney 1998). Cary and Banks (1999) use equations and inputs designed to
94 simulate fire in Australian fuels, and Perera *et al.* (2008) use equations and inputs designed for
95 fire simulation in Canadian boreal forest, complementing our study of southern California
96 shrublands. Additionally, FIRE-BGC (Keane *et al.* 1996) incorporated FARSITE (Finney 1998)
97 fire spread simulations into their model, though they only simulated the spread of two fires
98 within the 200 year simulation time frame, due to the inherent low fire return interval of their fire
99 regime. The remaining five models used simplified fire spread equations of unspecified
100 accuracy.

101 *HFire*

102 HFire is a spatially explicit, raster-based model of fire growth that incorporates the Rothermel
103 equations (Rothermel 1972, 1983) for fire spread. The Rothermel equations were developed
104 through burning small test fires in idealized dead fuels; from these experiments, equations were
105 developed to predict fire spread based upon weather, topography, and both live and dead fuel

106 amounts and properties. The Rothermel equations are frequently implemented in fire spread
107 models for use in intermediate spatial and temporal resolution fire spread simulations, such as
108 FARSITE (Finney 1998) which is operationally used by the US National Park Service and the
109 US Forest Service in both live and dead fuels (Pastor *et al.* 2003). Additionally, numerous
110 authors have utilized fire models that use the Rothermel equations to model landscapes including
111 live fuels, finding predictions of fire spread to be reasonable (e.g., Davis and Burrows 1994,
112 Arca *et al.* 2007, Dasgupta *et al.* 2007, Peterson *et al.* 2009), especially when appropriate custom
113 fuel models (Weise and Regelbrugge 1997, Arca *et al.* 2007, Peterson *et al.* 2009) are used.

114 HFire can be used to simulate individual fires or long-term fire regimes (Peterson *et al.*
115 2009). The computational efficiencies built into HFire allowed us to perform 1440 fire regime
116 simulations, each 1200 years long, for a 100 000 ha shrubland landscape in southern California.
117 HFire code can be found at the website of the model (<http://firecenter.berkeley.edu/hfire/>). Inputs
118 necessary for modeling an individual event in HFire are nearly identical to those for the widely
119 used FARSITE fire spread simulator (Finney 1998): ignition location(s); temporally varying
120 inputs such as wind speed and direction, and live and dead fuel moistures; and digital maps of
121 topography and fuel type. One-dimensional predictions from the Rothermel (1972) equations are
122 fit to two dimensions, using the solution to the ‘fire containment problem’ (Albini and Chase
123 1980) and the empirical double ellipse formulation of Anderson (1983). The raster
124 implementation utilized by HFire does not produce fractal/unrealistic fire perimeters as earlier
125 raster models did. This is demonstrated through a series of simulations comparing FARSITE and
126 HFire fire perimeters on both simplified and actual landscapes (Peterson *et al.* 2009). HFire uses
127 an adaptive time step, allows fire to spread into a cell from all neighboring cells over multiple

128 time steps, and is computationally efficient - a crucial advantage in long-term simulation studies
129 like those presented here (Peterson *et al.* 2009).

130 When HFire is used to simulate fire regimes, it implements the same fire spread
131 algorithm and landscape inputs as in individual event mode, with additional variables accounting
132 for stochastic ignitions, stochastic weather variables, stochastic LFM trend, and vegetation
133 growth/succession. It runs at an hourly time step between fires and at sub-minute intervals during
134 fires, for hundreds to thousands of simulated years.

135 Fires cannot occur without ignitions. The average number of ignitions per year and the
136 spatial distribution of ignitions are user-specified in HFire. Ignition probabilities can be spatially
137 homogeneous or based on landscape features, such as the distance to the nearest road for fire
138 regimes where anthropogenic ignitions are prevalent, or elevation for fire regimes where
139 lightning strikes are the primary source of ignitions (Keeley and Fotheringham 2003). The actual
140 number and location of these ignitions each year are then stochastically generated during the
141 simulation runs. Ignitions that do not result in a spreading fire are identified with a size threshold
142 parameter, and are not included in fire size statistics.

143 Weather is considered to be the most important variable for predicting how a fire will
144 spread for many ecosystems, including California chaparral (Davis and Michaelsen 1995, Moritz
145 1997). HFire uses hourly weather data (wind speed and direction, 10 h dead fuel moisture) to
146 model fire spread. 10 h dead fuel moisture is commonly used to estimate 1 h and 100 h dead fuel
147 moisture because 10 h data is measured at weather stations (Burgan *et al.* 1998). Weather data
148 files are populated with historical data from weather stations within the study area. A majority of
149 the total area burned in southern California occurs under extreme wind conditions, locally known
150 as Santa Ana wind conditions (Countryman 1974), so HFire was designed to accommodate

151 separate ‘standard’ and ‘extreme’ hourly weather inputs. The user specifies the annual average
152 number and duration of extreme fire weather events per year, with the timing and actual number
153 of extreme events per year stochastically determined by HFire. The weather values used at any
154 given hour during the simulation period are randomly selected from the standard or extreme data
155 files.

156 Live fuel moisture varies predictably on an intraannual basis, however it is highly
157 variable on an interannual basis due to differences in annual precipitation (Countryman and Dean
158 1979; Peterson *et al.* 2008). For fire regime simulations, woody and herbaceous LFM values are
159 stochastically simulated, given annual average values and standard deviations, and seasonal
160 trends. Bi-weekly LFM data are available from government agencies for many regions, LFM can
161 also be predicted using satellite data (Peterson *et al.* 2008).

162 Post-fire vegetation progresses through a series of fuel classes, represented by standard
163 and custom fuel models (Albini 1976; Weise and Regelbrugge 1997), until it burns again. A
164 climax, potential natural vegetation (PNV) type map is used to assign a particular successional
165 trajectory to each pixel. Using pixel ages and regeneration trajectories, a fuel model map is
166 produced. As the simulation progresses, age is incremented annually, or set to zero if the pixel
167 burns, and the per-pixel fuel models change accordingly. More detail on parameterizing
168 ignitions, weather, and vegetation regrowth is provided in the Methods section.

169 Fires go out naturally when they encounter conditions that slow them to the point of
170 extinction (e.g., moist or sparse vegetation), or they may be actively suppressed. Fire propagation
171 in a given HFire cell is stopped when the rate of spread drops below an extinction rate of spread
172 (ERS) threshold. After preliminary runs of HFire, we chose a baseline ERS threshold of 0.05 m
173 s⁻¹. This estimate is based on discussions with various Forest Service personnel, other fire

174 simulation work in southern California chaparral shrublands (e.g., Davis and Burrows 1994), and
175 comparison of preliminary model output (e.g., fire sizes, shapes, frequencies) with mapped fire
176 history for the Santa Monica Mountains (SMM). Other LFSMs have used a similar technique to
177 extinguish fires, basing the threshold on intensity (Cary and Banks 1999; Miller and Urban 2000)
178 or dead fuel moisture content (Perera *et al.* 2008) as opposed to rate of spread.

179 HFire model accuracy and sensitivity have been evaluated in single-event mode by
180 comparing observed and predicted fire spread during historical events (Peterson *et al.* 2009) and
181 for simulated landscapes (Clark *et al.* 2008; Peterson *et al.* 2009). HFire has also been utilized
182 previously in a comparison of empirical fire data, modeled fire regimes, and highly optimized
183 tolerance (HOT) as the mechanism for ecosystem structure in fire prone areas (Moritz *et al.*
184 2005).

185

186 **Methods**

187 *Study area, fuel characteristics, and vegetation dynamics*

188 The simulation domain for this project was a 96 000 ha region encompassing the Santa Monica
189 Mountains National Recreation Area (SMM), abutting the Pacific Ocean and the densely
190 populated Los Angeles metropolitan area in southern California (Fig. 1). The study area has a
191 Mediterranean-type climate characterized by hot, dry summers and cool, wet winters. Average
192 annual precipitation ranges from 400 mm at the coast to 600 mm at the mountain crest (Radtke *et*
193 *al.* 1982), and exhibits a high degree of both intra- and interannual variability (Keeley 2000; NPS
194 2005). Topography is rugged, with mountain peaks over 500 m in height just a few kilometers
195 inland from sea level (Fig. 1a). SMM is dominated by sclerophyllous, fire-dependent chaparral
196 and drought-deciduous coastal scrub shrublands, although there are also riparian corridors,

197 patches of invasive annual grasses, and vegetation typical of the local WUI (e.g., mixed native
198 and non-native landscaping) (Radtke *et al.* 1982; NPS 2005).

199 Fires in southern California shrublands tend to be stand-replacing, all aboveground
200 vegetation is killed (Keeley 2000). Herbaceous vegetation is dominant the first year after the fire,
201 with shrubs again becoming dominant three to five years after the fire (Horton and Kraebel 1955;
202 Keeley 2000). Shrub recovery comes from basal resprouting and/or seedling recruitment from
203 the pre-fire seed bank (Keeley 2000).

204 Spatial fuels data for the entire SMM area were derived from a 100 m X 100 m (1 ha)
205 resolution regional PNV map (Franklin 1997), which represents the vegetation community, and
206 therefore fuel type, that would occur in the long absence of fire. The PNV map was modified
207 using SMM maps of riparian areas and local planning agency maps of recent housing
208 development. Vegetation communities of the PNV map (Fig. 1b) capable of carrying wildfire
209 during typical weather conditions were then crosswalked to 1 of the 13 standard fuel models
210 (Albini 1976) or to custom fuel models for southern California shrubland vegetation (Weise and
211 Regelbrugge 1997). Vegetation types and their associated fuel models are shown in Table 1, and
212 details of the fuel models are summarized in online appendix Table A1
213 (<http://firecenter.berkeley.edu/hfire/>).

214 The progression of fuels after a fire depends on the local PNV type. Some types
215 regenerate on an annual basis, such as grass-dominated areas (NPS 2005) and others remain
216 relatively constant (e.g., WUI type). Most vegetation, however, is allowed to develop toward its
217 late successional PNV type, being progressively assigned fuel models that reflect accumulating
218 biomass and larger stem diameters (Table A1). The initial fuel model map was generated using
219 the initial stand age (from fire history of SMM as of 1999) and PNV maps.

220 *Factors that determine the fire regime*

221 Long-term fire regime sensitivity to the following four variables was evaluated: the number of
222 ignitions per year, the spatial pattern of ignitions, the number of Santa Ana events per year, and
223 LFM trend. Baseline settings for these variables are discussed below. HFire was run at 1 ha pixel
224 resolution for fuels and other spatial inputs, leading to an 870 x 300 pixel modeling domain.
225 Simulations were 1200 years long, but the first 200 years of each run were discarded to address
226 possible sensitivities to initial conditions, leaving 1000 years of simulated fires for analysis. Fire
227 spread was modeled for the period from July 1 to November 30 each year, the period of high fire
228 risk for southern California (NPS 2005). In fact, 70% of the historical fires recorded in SMM,
229 and 83% of the area burned, occurred between July 1 and November 30 (R. Taylor, pers.
230 comm.).

231 The mapped fire history for SMM is incomplete in the early 1900s (R. Taylor, pers.
232 comm.), so it was not possible to estimate reliable annual average ignition frequencies from this
233 dataset. The southern portion of the Los Padres National Forest (LPNF), however, is a nearby
234 shrubland-dominated region with a relatively complete ignition and fire perimeter record (Moritz
235 1999), providing rough estimates of ignition frequencies per unit area. On average, shrublands
236 of LPNF experienced a total of 0.37 ignitions per km² over the period 1911-1995. Therefore, for
237 a region the size of SMM (960 km²), a baseline estimate of 4.0 ignitions per year was chosen.
238 Other values tested in the model runs were 1.0, 8.0, and 12.0 ignitions per year. Most ignitions
239 are not likely to propagate and become fires in reality, as they are extinguished by human
240 activity quickly or they go out before successfully igniting fuels that will promote further spread
241 (Perera *et al.* 2008). This is incorporated into the model with a failed ignition size parameter,
242 which was set to one pixel (i.e., fires must progress out of the initial pixel to be counted).

243 In addition, HFire allows the user to specify ignition location probabilities, for example
244 increased probabilities along roads (Fig. 1c). In the SMM, 155 of the 161 fires from 1981-2003
245 were anthropogenic in origin, the remaining six were due to lightning strikes (NPS 2005), and
246 anthropogenic ignitions have been shown to preferentially occur close to roads (Keeley and
247 Fotheringham 2003; Syphard *et al.* 2008). We tested (i) spatially homogeneous and (ii) spatially
248 correlated ignition probabilities. For the latter case we used a piece-wise linear function whereby
249 relative ignition probability was uniform at 1.0 up to 100 m from a road bed, and decreased to
250 0.1 at 1000m from the road bed.

251 Fire weather conditions can have a very strong influence on fire regimes, and this is
252 especially true for chaparral-dominated shrublands (Davis and Michaelsen 1995; Moritz 1997;
253 Keeley and Fotheringham 2003). We separated fire weather data from 1997-2007 from two
254 weather stations in SMM (Cheeseboro and Malibu) into either ‘standard’ or ‘extreme’ days, by
255 examining relative humidity, wind speed and wind azimuth data, and a list of Santa Ana days
256 determined by Raphael (2003). This resulted in 3000 days of hourly observations for standard
257 weather. The extreme fire weather dataset is 10% of this size, consisting of 276 days of hourly
258 observations. A polar plot was used to show wind speed and azimuth values for the standard
259 (black) and extreme (red) data sets (Fig. 2). Standard winds can blow from any direction, with
260 southwest winds (wind blowing from the southwest) generally having the highest windspeeds.
261 Extreme winds, with high wind speeds, generally blow from about 20 to 95 degrees. The lower
262 windspeeds in the extreme data set are due to: (1) lulls in the winds mid-event, and (2) HFire
263 requires the classification of weather data as standard or extreme on a daily basis rather than an
264 hourly one, thus incorporating standard weather conditions at the beginning and end of extreme
265 events.

266 The weather data stream used in the model switches from standard to extreme weather a
267 user-specified number of times, corresponding to the average number of Santa Ana events per
268 fire year, for a user-specified length of time. The 1997-2007 average Santa Ana frequency was
269 5.2 events, with a standard deviation of 1.2 within the July 1 – November 30 HFire simulation
270 period. Values tested in the model runs were averages of 0.0, 1.0, 2.0, 4.0, 8.0, and 16.0 Santa
271 Ana events per year. The average duration of an event was calculated from the 1997-2007
272 weather data to be 2.4 days.

273 Live fuel moisture, a measure of the water content of live vegetation, affects rate of
274 spread and ignition success (Countryman and Dean 1979). LFM is particularly important in the
275 shrublands of southern California as a large proportion (55-75%) of the biomass available to fires
276 is living, so fires will only propagate if LFM is low (Countryman and Dean 1979; Dennison *et*
277 *al.* 2008). Dennison *et al.* (2008) examined the fire history of the SMM and found that all large
278 fires occurred at a LFM below 77%. LFM is input in to HFire separately for woody and for
279 herbaceous fuels (Fig. 3). We used average values for Los Angeles County chaparral for woody
280 LFM and Los Angeles County coastal sage scrub (CSS) for herbaceous LFM. The data were
281 provided by the Los Angeles County Fire Department. LFM follows a sinusoidal trend annually,
282 with maximum values in early spring and minima in the fall. Three different LFM trends were
283 tested: the average trend (1982-2007) during (i) wet years and (ii) dry years, and (iii) a
284 temporally invariant trend (60% for woody fuels, 105% for herbaceous fuels) that might be used
285 if more detailed information was unavailable. It can be seen that the peak LFM for CSS is nearly
286 double that of chaparral, and that it occurs earlier in the year, due to CSS species having
287 shallower roots. The differences between the two are lessened during the HFire simulation period
288 of July 1 – November 30 (Fig. 3). The average standard deviations during the simulation period

289 (wet/dry) were (10.0/5.2) for woody LFM, (40.0/27.0) for herbaceous LFM, and (5.0/5.0) for the
290 temporally invariant trend.

291 *Analysis*

292 We examined three aspects of fire regimes: fire size distributions, FRI maps, and cumulative
293 total area burned. Sensitivity to two categorical and two continuous independent variables was
294 assessed: spatial ignition pattern (uniform, increased number of ignitions closer to roads), live
295 fuel moisture trend (wet, dry, constant value), ignition frequency (1.0, 4.0, 8.0, 12.0 per year),
296 and Santa Ana event frequency (0.0, 1.0, 2.0, 4.0, 8.0, 16.0 per year). Ten replicates of each
297 scenario were performed, varying the starting random number seed, in order to make the results
298 more robust. Hence, a total of 1440 (2 ignition pattern x 3 LFM x 4 ignition frequency x 6 Santa
299 Ana frequency x 10 replicates) 1200 year model runs were performed.

300 Analysis of covariance (ANCOVA) was performed on the total area burned, which was
301 transformed using the natural logarithm to make the data follow a normal distribution, similar to
302 Cary *et al.* (2006). Linear regression is used to test relationships between a continuous dependent
303 variable and continuous independent variables, analysis of variance (ANOVA) is used to test
304 relationships between a continuous dependent variable and categorical independent variables,
305 and ANCOVA allows for both continuous and categorical variables to be tested in the same
306 model. Tukey's honestly significantly different (HSD) post-hoc pairwise comparisons are used to
307 determine which levels of a categorical variable are significantly different once ANOVA
308 determines that the variable is significant. Statistical analysis was performed within the R free
309 software environment (R 2008).

310

311 **Results**

312 *Modeling the current fire regime*

313 Reasonable, baseline parameter settings (uniform ignitions, 4.0 ignitions per year, 4.0 Santa Ana
314 events per year, wet LFM) simulated a fire regime that is representative of general fire patterns
315 in SMM (Fig. 4). In the SMM 1910-2007 fire history, the highest fire frequency occurs at the
316 southern boundary (the mountain range adjacent to the Pacific Ocean), with the central southern
317 portion having the most fires. There is another region of high fire frequency in the north central
318 portion. Much of the east portion experienced zero to one fires in the period 1910-2007. Fig. 4
319 also shows the last 100 years of modeled fire history for 3 of 10 randomly selected HFire
320 baseline parameter runs. Patterns in the simulated fire histories are also present in the actual fire
321 history. All three model results show a greater number of fires in the southern part of the area,
322 two of the three show enhanced fire frequency in the north central region, and fire frequency is
323 reduced in the eastern portion of SMM.

324 A commonly used fire regime metric is the FRI, defined to be the average number of
325 years between fires. The average FRI of the 10 random baseline runs was 37.2 years for the wet
326 LFM trend and 21.4 years for the dry LFM trend (Table 2). These values envelop the published
327 value of 32 years for SMM, which experienced a mixture of wet and dry years in the 1910-2007
328 period (NPS 2005).

329 Plots of simulated (1000 years) and actual fire size distributions demonstrate that the
330 baseline parameter settings generated distributions that are similar in form to that of the
331 chaparral-dominated portions LPNF (Fig. 5), indicating that simulated fire regimes approximate
332 those observed in real shrubland ecosystems well. The distributions of fire sizes follow a power
333 law, characterized by many very small events extending broadly out to relatively few larger
334 events (Fig. 5; Moritz 1997; Moritz *et al.* 2005; Cui and Perera 2008). The LPNF shrubland

335 dataset represents a largely complete fire history that includes even very small events (Moritz,
336 1999). The data were originally compiled in 1997, and have been updated through 2007 by
337 including fires recorded by CAL FIRE (Moritz 1999; FRAP 2009). LPNF is 10 times larger than
338 SMM, but the fire record (1910-2007) is approximately 1/10th as long as the HFire simulation
339 period, so the number of fires recorded was comparable. The SMM fire history (R. Taylor, pers.
340 comm.) is also included on the plot (Fig. 5), showing the form of both historical chaparral
341 datasets is similar, despite the smaller number of fires and reduced large fire size, due to the
342 reduced size of the study area.

343 The large difference between median and mean fire sizes shown in Table 2 is also
344 consistent with a power-law fire size distribution. Other measures characterizing the simulated
345 baseline fire regime, such as the percentage of ignitions propagating to become fires and the
346 coefficient of variation (CV) in fire size, are also given in Table 2.

347 *Evaluating fire regime drivers*

348 This section examines changes in fire size distributions and maps of FRIs resulting from varying
349 ignition pattern and frequency, Santa Ana frequency, and LFM trend, as well as univariate
350 relationships between those independent variables and the natural logarithm of total burned area.
351 Linear regression results are provided for the continuous variables and ANOVA results are
352 provided for the categorical variables.

353 Fig. 6 shows the effect of varying the four independent variables on fire size
354 distributions. The distributions shown represent the sum of all of the fires from the 10 HFire runs
355 having a different random number seed. Baseline settings (uniform ignitions, 4.0 ignitions per
356 year, 4.0 Santa Ana events per year, wet LFM) were used for the variables that were held
357 constant in the simulations. Varying the number of Santa Ana events has minimal effect on the

358 total number of fires, and the size of the 10 largest fires, however the distribution of medium to
359 large fire sizes is very different (Fig. 6a). The size of the 1000th fire increases from
360 approximately 2000 ha for the 0.0 Santa Ana cases to 30 000 ha for the 16.0 Santa Anas per year
361 cases. Many more medium to large fires occur under more extreme weather conditions. Varying
362 the number of ignitions has a different effect. As the number of ignitions per year increases, the
363 number of fires increases (Fig. 6b). However, the fire size distribution lines cross in the figure,
364 and the 12.0 ignitions per year case has the lowest largest fire size, as previously burned areas
365 within the same fire season act as fire breaks for subsequent fires. The variability in fire size
366 distributions is lower for the remaining two variables. Dry LFM generally leads to larger fires,
367 although the largest fires within the 1000 year modeling period are of similar size for the wet
368 LFM case (Fig. 6c). Having no set ignition pattern led to slightly larger intermediate fire sizes,
369 but the largest fires were of the same size (Fig. 6d).

370 The FRI maps show that spatial variability in FRI is high for all four independent
371 variables (Figs 7-9). The FRI maps presented here were constructed by averaging the FRI maps
372 from the 10 differently seeded HFire runs. Areas in red on the maps experience FRI less than 10
373 years, making them susceptible to type-conversion (Keeley *et al.* 2005). Fig. 7 shows the effect
374 of varying the number of Santa Ana events. As with Fig. 4a, which showed the fire history of the
375 past 100 years, Fig. 7 shows that the eastern and northerly western portions of the SMM burn
376 less regularly. The FRI decreases with increasing numbers of Santa Ana events, with only the far
377 eastern portion showing values greater than 100 years for the 16.0 Santa Ana events case. This is
378 to be expected as winds blow from the northeast during Santa Anas, and fires do not readily
379 spread upwind.

380 Fig. 8 shows the effect of varying the number of ignitions on FRI patterns. There is a
381 clear difference between the 1.0 and the 4.0, 8.0, and 12.0 ignitions per year maps. The central
382 southern portion of the landscape burns with return intervals of 30 years or less for the higher
383 number of ignitions cases but return intervals of 60 years or less for the one ignition per year
384 case.

385 Varying the LFM trend has a noticeable effect on FRI maps (Figs 9a, 9b, and 9c). The
386 three trends show similar spatial patterns of high and low values, with dry LFM having the
387 lowest FRI values, followed by wet and constant LFM. This is consistent with Fig. 6c, which
388 showed that large fires are most common for dry, then wet, then constant LFM.

389 The FRI maps for uniform and spatially correlated ignitions (Figs 9c and 9d) demonstrate
390 the importance of using multiple metrics to describe a fire regime. Fig. 6d showed minimal
391 differences in fire size distribution due to the spatial pattern of ignitions, but the FRI maps show
392 clear differences. The northerly western and the eastern portion of SMM show FRIs greater than
393 100 years in the uniform ignition pattern map (Fig. 9c), and there is a strong contrast with the
394 shorter FRIs seen in the central portion of SMM (FRI between 10 and 20 years). However, roads
395 are concentrated in the northerly western and eastern portions of SMM (Fig. 1c), and while FRI
396 is still highest in these portions of SMM for the correlated ignition pattern map, the area of FRI
397 greater than 100 years is reduced (Fig. 9d). The area of FRI between 10 and 20 years is also
398 reduced, leading to less contrast in values. It is interesting that introducing spatially correlated
399 ignitions serves to decrease the spatial variability evident in the FRI map.

400 Box plots showing relationships between the natural logarithm of total area burned and
401 the four independent variables are provided in Fig. 10. Increasing the number of ignitions
402 increases the total area burned, with the biggest increase occurring from 1.0 to 4.0 ignitions per

403 year (Fig. 10a). Increasing the number of Santa Ana events also shows increased total area
404 burned, though the relationship is more consistent (Fig. 10b). For LFM trend, dry conditions lead
405 to a much larger total area burned than the wet and constant trends (Fig. 10c). For ignition
406 pattern, uniform ignitions lead to a slightly larger total area burned (Fig. 10d).

407 Statistical tests demonstrate that the variability seen in the fire size distributions, FRI
408 maps, and box plots is very unlikely to arise by chance. All four of the independent variables
409 showed statistically significant relationships with the logarithm of total area burned ($p < .0001$),
410 with number of ignitions explaining the most variance ($R^2 = 0.395$, slope = 0.175, intercept =
411 13.74, Table 3), followed by number of Santa Anas ($R^2 = 0.327$, slope = 0.12, intercept = 14.21),
412 LFM trend ($R^2 = 0.08$), and spatial ignition pattern ($R^2 = 0.008$). The number of ignitions had a
413 steeper slope than the number of Santa Anas and thus is more sensitive to total area burned. All
414 Tukey's HSD posthoc pairwise comparisons for LFM were significantly different ($p < 0.05$),
415 though wet and constant were not also significantly different at the .001 level.

416 *Multivariate relationships*

417 The cumulative variance explained by the four independent variables, without interactions, was
418 0.8094 (Table 3). All possible interaction terms were added, and then non-significant terms were
419 removed in a stepwise manner using the Akaike information criteria (AIC: Akaike 1974). When
420 the statistically significant interaction effects were included, the explained variance increased to
421 0.8702 (Table 3). Four interactions were significant at the 0.0001 level: between LFM trend and
422 the number of Santa Anas, LFM trend and the number of ignitions, number of ignitions and the
423 number of Santa Ana events, and the interaction between these three variables. The implications
424 of these interaction terms are discussed below.

425 Most of the area burned in chaparral shrublands is during Santa Ana events in actuality
426 (Countryman 1974) and also in HFire. Intuitively, increasing the number of ignitions increases
427 the chances that an ignition will occur coincident with a Santa Ana event, up to a point. This may
428 be the mechanism for the importance of the interaction between annual numbers of Santa Ana
429 events and ignitions. One of the text outputs from HFire lists area burned under standard and
430 extreme conditions, for each fire. Fig. 11 shows a contour plot representing the percentage of
431 area burned during extreme conditions as a function of number of ignitions and Santa Anas. A
432 number of interesting trends are present in the plot. For lower numbers of Santa Anas per year
433 (0.0, 1.0, 2.0), the percent area burned during a Santa Ana does not change when the number of
434 ignitions increases. Once the number of Santa Ana events per year is 4.0 or greater, increasing
435 the number of ignitions results in increasing percent area burned during a Santa Ana from 0.450
436 to 0.6 – 0.8. For high numbers of both ignitions and Santa Anas, the number of Santa Anas is
437 more sensitive to Santa Ana fraction of total area burned than number of ignitions. This suggests
438 that the system is more limited by the number of wind events rather than the number of ignitions.
439 The FRI maps for the ignitions per year cases also show that once ignitions increase beyond 1.0
440 per year, FRI remains fairly consistent (Fig. 8).

441 In the interaction between LFM and the number of Santa Ana events per year, it is clear
442 that the constant trend has the steepest slope and thus is most sensitive to the number of Santa
443 Anas (Fig. 12). The wet LFM trend shows a slightly steeper slope than the dry LFM trend,
444 suggesting that wetter fuels require more wind than drier fuels in order to burn larger amounts of
445 the landscape. The disparity in slope between the constant and wet/dry LFM trends is due to the
446 smaller amounts of total area burned for the lower Santa Ana events per year cases for the
447 constant trend, LFM may have been above a threshold that would lead to large fires under low

448 wind conditions. It is interesting to note that for the zero Santa Ana case, the fire risk in the
449 system appears to be fuel dominated as the dry LFM trend produces larger fires than the wet and
450 constant trends. But as more Santa Anas are added, the differences in area burned due to LFM
451 trend are reduced (all three LFM trends lead to a mean natural logarithm of total area burned of
452 roughly 16 when the number of Santa Ana events per year increased to 16.0).

453 The interaction between LFM and the number of ignitions per year shows some similar
454 patterns. All three trends show a large jump in area burned between the one and four ignitions
455 per year cases, and the constant trend shows the steepest slope overall (Fig. 13). However it is
456 interesting to note that the three different LFM trends have less similar values for the maximum
457 number of ignitions per year than they showed for the maximum number of Santa Anas per year
458 (Fig. 13). The Santa Ana variable was able to dominate the effect of the LFM variable more so
459 than the number of ignitions variable did.

460

461 **Discussion**

462 We studied drivers (weather, ignition, and fuel) of the long-term fire regime of SMM using the
463 HFire LFSM. Three different aspects of the fire regime were examined: the distribution of fire
464 sizes, the cumulative total fire size, and the spatial patterns of the FRI. These three ways of
465 visualizing the output are complimentary, with the maps providing the most detail, and boxplots
466 of the total area burned able to efficiently summarize a large number of model runs.

467 The number of ignitions was most important for predicting total area burned.
468 Haydon *et al.* (2000) also found high model sensitivity to varying the number of ignitions,
469 especially when values more than +/- 100% different were tested. In contrast, Oliveras *et al.*
470 (2005) showed minimal sensitivity when the number of ignitions varied between 26 and 110 per

471 year, corresponding to half to two times the current fire ignition frequency per year for their
472 study area. For our data, if we remove the one ignition per year model runs, which are one
473 quarter the current fire ignition frequency of four per year, the R^2 for this variable drops from
474 0.395 to 0.138, though this value is still significant. Hence, while increasing the number of
475 ignitions from 4.0 to 12.0 still serves to increase the total area burned, model sensitivity is
476 reduced. A possible explanation is that within a calendar year, prior fires in the fire season may
477 act as fire breaks to later fires, so that more ignitions does not necessarily equate to more area
478 burned. The fire size distribution plot (Fig. 6b) and FRI map (Fig. 8) for the number of ignitions
479 variable support the idea that the biggest difference in fire properties occurs from 1.0 to 4.0
480 ignitions, with the 4.0, 8.0, and 12.0 ignition cases having more similar output.

481 This has implications for future fire regimes because ignitions preferentially occur in
482 WUI areas (Radeloff *et al.* 2005, Syphard *et al.* 2007), and the WUI will expand in coming
483 decades (Swenson and Franklin 2000). From our model results, it would appear that the
484 increased number of ignitions beyond the current value will have a small effect on burned area.
485 However, increased numbers of people living in the WUI will lead to increased exposure to fire.

486 The number of Santa Ana events also explained a large amount of variance in total area
487 burned. When the 1.0 ignition per year model runs were removed from the analysis, the R^2 for
488 number of Santa Anas increased from 0.327 to 0.571 and the overall R^2 increased from 0.809 to
489 0.832. Additionally, the Santa Ana variable shows the most consistent increase in area burned in
490 Fig. 6, and the most consistent decrease in FRI in Figs 7-9. This finding heightens the value of
491 initial fire suppression efforts when Santa Ana events are forecast, especially during dry years, if
492 a commensurate increase in total area burned, and loss of life and structures is to be avoided
493 (Westerling *et al.* 2004).

494 The importance of weather-related factors is well established in the fire modeling
495 literature (e.g., Cary *et al.* 2006). Additionally, a global sensitivity analysis applied to HFire in
496 single-event mode found that windspeed was three times as important as the second place input
497 (1 h dead fuel moisture) for predicting fire size (Clark *et al.* 2008).

498 Climate change is likely to have major effects on ecosystem structure and function, and
499 changing fire regimes will play an important role on many terrestrial landscapes. General
500 circulation models (GCMs) are typically used to predict changes in average temperature and
501 precipitation rather than extreme weather events, but two recent studies have examined changes
502 in Santa Ana event frequencies under different climate change scenarios (Miller and Schlegel
503 2006; Hughes *et al.* 2009). Miller and Schlegel (2006) predicted that the peak Santa Ana season
504 will shift from September-October to November-December by the end of the 21st century.
505 Hughes *et al.* (2009), using a different GCM and methodology, show that Santa Ana frequency
506 has decreased 30% from the 1960s to the 1990s and predict a similar decrease through the mid
507 21st century. The impact of the number of Santa Ana events on fire regime evident in our
508 research provides impetus for clarifying the response of Santa Ana frequency to climate change.

509 The sensitivity to LFM trend in HFire is reflected in actual conditions, too. Weise *et al.*
510 (1998) suggested that fire danger can be approximated using LFM, with low fire danger for LFM
511 > 120%, moderate fire danger for 120% > LFM > 80%, high fire danger for 80% > LFM > 60%,
512 and extreme fire danger for LFM < 60%. The dry LFM trend has values at 60% for August,
513 September, and October, whereas LFM does not reach 60% for the wet trend. Dennison *et al.*
514 (2008) also found an interaction between LFM and Santa Ana events. They found that the seven
515 largest fires in the SMM between 1982 and 2007 occurred when the LFM was below 77%, and
516 Santa Ana winds were present. The net effect of climate change predictions on LFM are unclear,

517 as winter and summer temperatures are predicted to increase by 3⁰C and 1⁰C, respectively, which
518 would tend to dry out fuels, but precipitation is also expected to increase, which may increase
519 LFM (Field *et al.* 1999). If future fuels are drier, the fire regime will shift to more, larger fires,
520 with a shorter return interval.

521 The pattern of ignitions demonstrates that viewing different aspects of the fire regime
522 may reveal different trends. The fire size distribution and the total burned area both show
523 minimal differences due to uniform and spatially correlated ignitions. However, the two FRI
524 maps show clear differences. The uniform ignitions map has more areas of high and low FRI,
525 whereas the correlated ignitions map has less contrast.

526 It is doubtful that native plant species which dominate many shrublands of California will
527 be able to persist under shorter fire return intervals, because for many fire-dependent chaparral
528 species, there is a threshold in fire return interval below which plants are not able to successfully
529 regenerate (Zedler *et al.* 1983). Large areas of FRI below 10 years (highlighted in red in Figs 7-
530 9) occurred in HFire simulations under three conditions: when the number of Santa Ana events
531 was 16.0 per year, when ignitions increased to 12.0 per year, and under dry LFM conditions. The
532 16.0 Santa Ana per year case is plausible, but unlikely, given current climate change predictions
533 (Miller and Schlegel 2006; Hughes *et al.* 2009). Future LFM trends are unclear, as discussed
534 above. However, increasing ignitions are almost certain to occur as the WUI expands (Syphard *et*
535 *al.* 2007), so there is a risk of type-conversion in the future. Additionally, once a threshold is
536 crossed and native vegetation is type-converted into non-native invasive grasses, further
537 alterations to vegetation patterns and fire regimes are likely through positive feedback cycles
538 (D'Antonio and Vitousek 1992).

539

540 **Conclusions**

541 Fire regimes are characterized by statistics describing fire size distributions, fire return intervals,
542 and cumulative total area burned. HFire has been shown to model the fire regime of a southern
543 California shrubland (Moritz et al. 2005). In this paper we evaluated the importance of four
544 physical drivers of these characteristics for southern California. These include the annual number
545 of ignitions, the spatial pattern of ignitions, the annual number of Santa Ana wind events, and
546 live fuel moisture trends. Our simulations demonstrated the most significant change in the fire
547 regime metrics arose in response to variations in ignition frequency and extreme fire weather
548 events, while fuel moisture trend and ignition pattern had less influence on fire regime metrics.
549 Not surprisingly, the largest cumulative area burned occurred under the most ignitions (12.0 per
550 year), highest wind (16.0 Santa Anas per year), most flammable fuels (dry LFM trend) scenario.

551 This study demonstrates the promise of HFire as an efficient, mechanistic fire model for
552 long-term fire regime studies. This paper examined steady state fire regimes for a range of values
553 of the drivers. This provides an initial means to evaluate how fire regimes may change in
554 response to changes in the drivers. More detailed studies of specific scenarios could be obtained
555 by extracting estimates of time varying drivers from models of climate change or urbanization,
556 which could provide projections for changes in weather parameters, fuel conditions, and
557 ignitions, which could then be used as time varying inputs for HFire.

558 Incorporation of possible vegetation type conversion (e.g., stochastically driven changes
559 in PNV type based on fire frequency at a site) represents a top priority for the next stage of
560 model development, and will aid in these studies of long term change. Additionally, more
561 complex variations in fuel model pathways will be explored, involving more chaparral fuel
562 models. Several dynamical upgrades are also of interest. Spotting can increase the overall spread

563 rate of a fire across a landscape, and this has been observed in fire simulation modeling studies
564 (Hargrove et al. 2000). We expect spotting will play an important role in the dynamics of
565 individual fires, including mechanisms for spread of fires into urban areas, but may not have a
566 major impact on long term statistical metrics. Many potential spot fires are eventually overtaken
567 by the main fire, so that the majority of short-range spotting may not have a major cumulative
568 effect on final fire size (Rothermel 1983), and hence fire size distributions/fire regimes. In
569 addition, upgrades which expand the range of fire regimes which can be investigated are of
570 interest. HFire was developed to model stand-replacing fires in shrubland fuels and thus HFire
571 does not currently model the local, vertical transition of surface fire to crown fire in a forest
572 canopy. As such, the general relationships between physical parameters and fire regimes we
573 observed may or may not hold in ecosystems where this local transition has a large effect on
574 landscape-scale spatial fire patterns and long-term fire regime dynamics.

575 Modeling is one of few approaches available for investigating fire regime dynamics
576 under future climate change and WUI expansion scenarios. New tools like HFire are useful for
577 exploring sensitivities and possible future scenarios, where the physical parameters governing
578 fire spread are expected to change. Detailed and physically-based fire growth algorithms are
579 often considered too complex and computationally intensive for long-term simulations, but
580 HFire's implementation of the Rothermel (1972) equations allows for multi-century modeling of
581 fire regimes, with simultaneous fires burning on a landscape and regrowth of vegetation between
582 fires.

583 **Acknowledgements**

584 Sincere thanks to Robert S. Taylor, Biogeographer/Fire GIS Specialist, Santa Monica Mountains
585 National Recreation Area, for compiling and providing fire history data for the park.

586 This work was supported by the David and Lucile Packard Foundation, the James S. McDonnell
587 Foundation, the Institute for Collaborative Biotechnologies through grant DAAD19-03-D-0004
588 from the U.S. Army Research Office, and the Office of Naval Research through grant ONR
589 MURI N000140810747.

590

591 **References**

592 Albin FA (1976) 'Estimating wildfire behavior and effects.' USDA Forest Service,
593 Intermountain Forest and Range Experiment Station General Technical Report GTR-
594 INT-30. (Ogden, UT)

595 Albin FA, Chase CH (1980) 'Fire containment equations for pocket calculators.' USDA Forest
596 Service, Intermountain Forest and Range Experiment Station Research Paper RP-INT-
597 268. (Ogden, UT)

598 Akaike H (1974) A new look at statistical model identification. *IEEE Transactions on Automatic*
599 *Control* **19**, 716-723.

600 Anderson HE (1983) 'Predicting wind-driven wildland fire size and shape.' USDA Forest
601 Service, Intermountain Forest and Range Experiment Station Research Paper RP-INT-
602 305. (Ogden, UT)

603 Arca B, Duce P, Laconi M, Pellizzaro G, Salis M, Spano D (2007) Evaluation of FARSITE
604 simulator in Mediterranean maquis. *International Journal of Wildland Fire* **16**, 563-572.

605 Burgan RE, Klaver RW, Klaver JM (1998) Fuel models and fire potential from satellite and
606 surface observations. *International Journal of Wildland Fire* **8**, 159-170.

607 Cary GJ, Banks, JCG (1999) Fire regime sensitivity to global climate change: an Australian
608 perspective. In 'Advances in Global Change Research: Biomass Burning and its Inter-
609 Relationships with the Climate System'. (Eds JL Innes, M Beniston, MM Verstraete) pp.
610 233-246. (Kluwer Academic Publishers: London)

611 Cary GJ, Keane RE, Gardner RJ, Lavorel S, Flannigan MD, Davies ID, Li C, Lenihan JM, Rupp
612 TS, Mouillot F (2006) Comparison of the sensitivity of landscape-fire-succession models
613 to variation in terrain, fuel pattern, climate and weather. *Landscape Ecology* **21**, 121-137.

614 Clark RE, Hope AS, Tarantola S, Gatelli D, Dennison PE, Moritz MA (2008) Sensitivity
615 analysis of a fire spread model in a chaparral landscape. *Fire Ecology* **4**, 1-13.

616 Countryman, C.M. (1974). 'Can southern California wildland conflagrations be stopped?' USDA
617 Forest Service, Pacific Southwest Forest and Range Experiment Station General
618 Technical Note GTN-PSW-7. (Berkeley, CA)

619 Countryman CM, Dean WH (1979) 'Measuring moisture content in living chaparral: A field
620 user's manual'. USDA Forest Service, Pacific Southwest Forest and Range Experiment
621 Station General Technical Report GTR-PSW-36. (Berkeley, CA)

622 Cui W, Perera AH (2008) What do we know about fire size distribution, and why is this
623 knowledge useful for forest management? *International Journal of Wildland Fire* **17**,
624 234-244.

625 D'Antonio CM, Vitousek PM (1992) Biological invasions by exotic grasses, the grass-fire cycle,
626 and global change. *Annual Review of Ecology and Systematics* **23**, 63-87.

627 Dasgupta S, Qu JJ, Hao X, Bhoi S (2007) Evaluating remotely sensed live fuel moisture
628 estimations for fire behavior predictions in Georgia, USA. *Remote Sensing of*
629 *Environment* **108**, 138-150.

630 Davis FW, Burrows DA (1994) Spatial simulation of fire regime in Mediterranean-climate
631 landscapes. In 'The Role of Fire in Mediterranean-type Ecosystems'. (Eds JM Moreno,
632 WC Oechel) pp. 117-139. (Springer: New York)

633 Davis FW, Michaelsen J (1995) Sensitivity of fire regime in chaparral ecosystems to climate
634 change. In 'Global Change and Mediterranean-type Ecosystems'. (Eds JM Moreno, WC
635 Oechel) pp. 203-224. (Springer: New York)

636 Dennison PE, Moritz MA, Taylor RS (2008). Examining predictive models of chamise critical
637 live fuel moisture in the Santa Monica Mountains, California. *International Journal of*
638 *Wildland Fire* **17**, 18–27.

639 Field CB, Daily GC, Davis FW, Gaines S, Matson PA, Melack J, Miller NL (1999) Confronting
640 climate change in California: Ecological impacts on the golden state. (Union of
641 Concerned Scientists: Cambridge, MA and Ecological Society of America: Washington,
642 D.C.)

643 Finney MA (1998) 'FARSITE: Fire Area Simulator- model development and evaluation'. USDA
644 Forest Service, Rocky Mountain Research Station Research Paper RP-RMRS-4. (Ft.
645 Collins, CO)

646 Franklin J (1997) Forest Service Southern California Mapping Project: Santa Monica Mountains
647 National Recreation Area, Final Report. 11p. Unpublished report.

648 Franklin J, Syphard AD, Mladenoff DJ, He HS, Simons DK, Martin RP, Deutschman D,
649 O'Leary JF (2001) Simulating the effects of different fire regimes on plant functional
650 groups in southern California. *Ecological Modelling* **142**, 261-283.

651 FRAP 2009. 'Fuels: Surface Fuels.' Available at
652 <http://frap.cdf.ca.gov/data/frapgisdata/select.asp?theme=5> [Verified 15 September 2009]

653 Hargrove WW, Gardner RH, Turner MG, Romme WH, Despain DG (2000) Simulating fire
654 patterns in heterogeneous landscapes. *Ecological Modeling* **135**, 243-263.

655 Haydon DT, Friar JK, Pianka ER (2000) Fire-driven dynamic mosaics in the Great Victoria
656 Desert, Australia. *Landscape Ecology* **15**, 407-423.

657 Horton JS, Kraebel CJ (1955) Development of vegetation after fire in the chamise chaparral of
658 southern California. *Ecology* **36**, 244-262.

659 Hughes M, Hall A, Kim J (2009) Anthropogenic reduction of Santa Ana winds. '2008 Climate
660 Change Impacts Assessment Project, Second Biennial Science Report to the California
661 Climate Action Team'. CEC-500-2009-015-D. 19 pp.

662 Keane RE, Ryan KC, Running SW (1996) Simulating effects of fire on northern Rocky
663 Mountain landscapes with the ecological process model FIRE-BGC. *Tree Physiology* **16**,
664 319-331.

665 Keane RE, Finney MA (2003) The simulation design for modeling landscape fire, climate,
666 ecosystem dynamics. In 'Fire and Climatic Change in Temperate Ecosystems of the
667 Western Americas'. (Eds TT Veblen, WLBaker, G Montenegro, TW Swetnam) pp.32-68.
668 (Springer: New York)

669 Keane RE, Cary GJ, Davies ID, Flannigan MD, Gardner RJ, Lavorel S, Lenihan JM, Li C, Rupp
670 TS (2004) A classification of landscape fire succession models: spatial simulations of fire
671 and vegetation dynamics. *Ecological Modelling* **179**, 3-27.

672 Keeley JE (2000) Chaparral. In 'North American Terrestrial Vegetation, 2nd Edition'. (Eds MG
673 Barbour, WD Billings) pp. 203-253. (Cambridge University Press: N.Y.)

674 Keeley JE, Fotheringham CJ (2003) Impact of past, present, and future fire regimes on North
675 American mediterranean shrublands. In 'Fire and Climatic Change in Temperate
676 Ecosystems of the Western Americas'. (Eds TT Veblen, WL Baker, G Montenegro, TW
677 Swetnam) pp. 218-262. (Springer: New York)

678 Keeley JE, Fotheringham CJ, Baer-Keeley M (2005) Determinants of postfire recovery and
679 succession in Mediterranean-climate shrublands of California. *Ecological Applications*
680 **15**, 1515-1534.

681 Mensing SA, Michaelsen J, Byrne R (1999) A 560-year record of Santa Ana fires reconstructed
682 from charcoal deposited in the Santa Barbara Basin, California. *Quaternary Research* **51**,
683 295-305.

684 Miller C, Urban DL (2000) Modeling the effects of fire management alternatives on Sierra
685 Nevada mixed-conifer forests. *Ecological Applications* **10**, 85-94.

686 Miller NL, Schlegel NJ (2006) Climate change projected fire weather sensitivity: California
687 Santa Ana wind occurrence. *Geophysical Research Letters* **33**, L15711.

688 Moritz MA (1997) Analyzing extreme disturbance events: fire in Los Padres National Forest.
689 *Ecological Applications* **7**, 1252-1262.

690 Moritz MA (1999) Controls on disturbance regime dynamics: Fire in Los Padres National Forest.
691 Ph.D. Dissertation. (University of California: Santa Barbara, CA)

692 Moritz MA, Morais ME, Summerell LA, Carlson JM, Doyle J (2005) Wildfires, complexity, and
693 highly optimized tolerance. *Proceedings of the National Academy of Sciences of the*
694 *United States of America* **102**, 17912-17917.

695 Moritz MA, Stephens SL (2008) Fire and sustainability: considerations for California's altered
696 future climate. *Climatic Change* **87** (Suppl 1), S265-S271.

697 National Park Service (2005) Final environmental impact statement for a fire management plan,
698 Santa Monica Mountains National Recreation Area. USDI, National Park Service.
699 (Thousand Oaks, CA)

700 Oliveras I, Piñol J, Viegas DX (2005). Modelling the long term effects of changes in fire
701 frequency on the total area burnt. *Orsis* **20**, 73-81.

702 Pastor E, Zárata L, Planas E, Arnaldos J (2003) Mathematical models and calculation systems
703 for the study of wildland fire behaviour. *Progress in Energy and Combustion Science* **29**,
704 139-153.

705 Perera AH, Ouellette M, Cui W, Drescher M, Boychuk D (2008) BFOLDS 1.0: A spatial
706 simulation model for exploring large scale fire regimes and succession in boreal forest
707 landscapes. Ontario Forest Research Institute Forest Research Report number 152. (Sault
708 Ste. Marie, Ontario)

709 Peterson SH, Roberts DA, Dennison PE (2008). Mapping live fuel moisture with MODIS data:
710 A multiple regression approach. *Remote Sensing of Environment* **112**, 4272-4284.

711 Peterson SH, Morais ME, Carlson JM, Dennison PE, Roberts DA, Moritz MA, Weise DR (2009)
712 'Using HFire for spatial modeling of fire in shrublands'. USDA Forest Service, Pacific
713 Southwest Research Station Research Paper PSW-RP-259 (Albany, CA)

714 R Development Core Team (2008). R: A language and environment for statistical computing. R
715 Foundation for Statistical Computing, Vienna, Austria. ISBN 3-900051-07-0, URL
716 <http://www.R-project.org> [Verified 15 September 2009]

717 Radeloff VC, Hammer RB, Stewart SI, Fried JS, Holcomb SS, McKeefry JF (2005) The
718 wildland-urban interface in the United States. *Ecological Applications* **15**, 799-805.

719 Radtke KWH, Arndt AM, Wakimoto RH (1982). Fire history of the Santa Monica Mountains.
720 USDA Forest Service, Pacific Southwest Forest and Range Experiment Station, General
721 Technical Report PSW-58 (Eds CE Conrad, WC Oechel) pp. 438–443. (Berkeley, CA)

722 Raphael MN (2003) The Santa Ana winds of California. *Earth Interactions* **7**, 1-13.

723 Rothermel RC (1972) ‘A mathematical model for predicting fire spread in wildland fuels.’
724 USDA Forest Service, Intermountain Forest and Range Experiment Station Research
725 Paper RP-INT-115. (Ogden, UT)

726 Rothermel RC (1983) ‘How to predict the spread and intensity of forest and range fires’. USDA
727 Forest Service, Intermountain Forest and Range Experiment Station General Technical
728 Report GTR-INT-143. (Ogden, UT)

729 Swenson JJ, Franklin J (2000) The effects of future urban development on habitat fragmentation
730 in the Santa Monica Mountains. *Landscape Ecology* **15**, 713-730.

731 Syphard AD, Radeloff VC, Keeley JE, Hawbaker TJ, Clayton MK, Stewart SI, Hammer RB
732 (2007) Human influence on California fire regimes. *Ecological Applications* **17**, 1388-
733 1402.

734 Syphard AD, Radeloff VC, Keuler NS, Taylor RS, Hawbacker TJ, Stewart SI, Clayton MK
735 (2008) Predicting spatial patterns of fire on a southern California landscape. *International*
736 *Journal of Wildland Fire* **17**, 602-613.

737 Venevsky S, Thonicke K, Sitch S, Cramer W (2002) Simulating fire regimes in human-
738 dominated ecosystems: Iberian Peninsula case study. *Global Change Biology* **8**, 984-998.

739 Weise DR, Hartford RA, Mahaffey L (1998) Assessing live fuel moisture for fire management
740 applications. In 'Fire in ecosystem management: Shifting the paradigm from suppression
741 to prescription' (Eds TL Pruden, LA Brennan) Tall Timbers Fire Ecology Conference
742 Proceedings, Vol. 20 (pp. 49–55). (Tall Timbers Research Station: Tallahassee, FL)

743 Weise DR, Regelbrugge JC (1997) Recent chaparral fuel modeling efforts. Resource
744 Management: The Fire Element (Newsletter of the California Fuels Committee). USDA
745 Forest Service, Pacific Southwest Research Station, Prescribed Fire and Fire Effects
746 Research Unit. 1p. (Riverside, CA).

747 Westerling AL, Cayan DR, Brown TJ, Hall BL, Riddle LG (2004) Climate, Santa Ana winds,
748 and autumn wildfires in southern California. *EOS* **85**, 289, 296.

749 Zedler PH, Gautier CR, McMaster GS (1983) The effect of a short interval between fires in
750 California chaparral and coastal scrub. *Ecology* **64**, 809-818.

Table 1. Vegetation, regrowth characteristics, and associated fuel models. These classes represent the mapped PNV types within the study area and their simplified paths of fuel regrowth after a fire. For classes that are assumed to accumulate biomass with age, fuel models change with time since fire, and the relevant time periods for each stage are given in parentheses. Both standard (Northern Forest Fire Laboratory, NFFL (Albini 1976)) and custom fuel model parameter estimates are provided in Online Appendix table A1 (<http://firecenter.berkeley.edu/hfire/>).

PNV vegetation type	Area (ha)	Immediately following fire	Early stage	Later stage
Agricultural	1461	Not burnable	Not burnable	Not burnable
Coastal dune scrub	844	Not burnable	Not burnable	Not burnable
Coastal strand	295	Not burnable	Not burnable	Not burnable
Riparian (NPS)	3431	Not burnable	Not burnable	Not burnable
Rock outcrops	201	Not burnable	Not burnable	Not burnable
Salt marsh	156	Not burnable	Not burnable	Not burnable
Unknown	19	Not burnable	Not burnable	Not burnable
Water	485	Not burnable	Not burnable	Not burnable
Non-native annual grass	3421	NFFL 1	NFFL 1	NFFL 1
Coastal cactus scrub	402	NFFL 1	NFFL 1	NFFL 1
Valley oak	474	NFFL 1	NFFL 1	NFFL 1
Walnut	127	NFFL 1	NFFL 1	NFFL 1
Coast live oak	1742	NFFL 3	NFFL 3	NFFL 3
Non-native conifer/hardwood	26	NFFL 9	NFFL 9	NFFL 9
Riparian (sycamore/oak)	678	NFFL 9	NFFL 9	NFFL 9
Chamise chaparral	1450	NFFL 5 (1-2 years)	Custom 17 (3-15 years)	Custom 15 (>16 years)
Red shank chaparral	322	NFFL 5 (1-2 years)	Custom 17 (3-15 years)	Custom 15 (>16 years)
Coastal scrub/chaparral mix	418	NFFL 5 (1-3 years)	Custom 21 (4-12 years)	Custom 16 (>13 years)
Northern mixed chaparral	36737	NFFL 5 (1-2 years)	Custom 18 (3-12 years)	Custom 16 (>13 years)
Coastal sage scrub	18922	NFFL 5 (1-3 years)	Custom 21 (4-15 years)	Custom 18 (>16 years)
Development (WUI)	24241	Custom 20	Custom 20	Custom 20

Table 2. Fire regime metrics for baseline parameter settings of HFire (aspatial ignitions, 4 ignitions per year, 4 Santa Ana events per year, wet LFM). Values for constant and dry LFM are also shown. Columns 2-7 indicate the following: number of actual ignitions simulated over the period analyzed; percentage of ignitions becoming fires; fire return interval, median fire size, mean fire size, and coefficient of variation (CV) in fire size.

Live fuel moisture trend	Total ignitions (#/1000 yr)	Become fires (%)	Fire return interval (yr)	Median fire size (ha)	Mean fire size (ha)	CV fire size (ha)
Constant	4014.2	44	49.2	53.4	1275.7	3.8
Wet	4030.0	40	37.2	41.7	1770.2	3.9
Dry	4003.1	48	21.4	116.7	2687.7	2.9

Table 3. Sum of squares and R^2 for the four independent variables (ig_pattern: categorical variable concerning ignition pattern, lfm: categorical variable concerning live fuel moisture trend used, sa: average annual number of Santa Ana events igpy: average annual number of ignitions) and the significant interactions on ln-transformed total area burned. All are significant at the .0001 level.

Independent variable(s)	Degrees of freedom	Sum of squares	R^2
ig_pattern	1	14.4	0.0075
lfm	2	153.4	0.0801
sa	1	625.6	0.3265
igpy	1	757.4	0.3953
lfm+sa	2	38.5	0.0201
lfm+igpy	2	69.0	0.0360
sa+igpy	1	3.4	0.0018
lfm+sa+igpy	2	5.5	0.0029
Residuals	1427	248.7	

Figure captions

Figure 1. Study area. The inset at top shows the location of the SMM study area along the coast of southern California. Points C and M indicate the locations of Cheeseboro and Malibu weather stations from which hourly weather data were obtained. Panel A demonstrates the patterns of topography in the study area. Panel B indicates aggregated vegetation class patterns in SMM (see Table 1 for detailed breakdown). Panel C indicates the road network and associated probabilities of ignition.

Figure 2. Polar plot showing historical (1997-2007) wind speed (miles per hour) and direction data under normal (black) and Santa Ana (red) conditions for the Cheeseboro and Malibu weather station, SMM.

Figure 3. Live fuel moisture trends (LFM) used in the HFire model runs, data derived from the Los Angeles County Fire Department LFM monitoring program.

Figure 4. Fire frequency for SMM, actual 1910-2007 (a), and the last 100 years of three randomly selected HFire runs (b-d) using baseline parameters (aspatial ignitions, 4 ignitions per year, 4 Santa Ana events per year, wet LFM).

Figure 5. Historical LPNF (black) and historical SMM (dashed black) vs. simulated (10 colored lines) HFire baseline parameterization fire size distributions. The historical LPNF dataset includes all chaparral fires in LPNF from 1911-1995 plus CAL FIRE data from 1996-2007. The historical SMM dataset covers 1910-2008 and contains all known fires. The historical datasets were subset to only include fires larger than 2 ha, the minimum fire size generated by HFire. The data were sorted by fire size in descending order (largest fire has a rank of 1).

Figure 6. Cumulative fire-size probability distributions, summing the 10 different random runs varying (a) the number of Santa Ana events per year (0, 1, 2, 4, 8, 16; red, green, blue, cyan, magenta, black), (b) the number of ignitions (1, 4, 8, 12; black, red, green, blue), (c) the Live Fuel Moisture (constant, wet, dry; black, red, green), and (d) the ignition pattern (no pattern, higher probability closer to roads; black, red). The data were sorted by fire size in descending order (largest fire has a rank of 1).

Figure 7. Fire Return Interval maps for 1000 years of fires for SMM, showing the effect of increasing the number of Santa Ana (SA) events from 0 to 16 per year. Other parameters held constant were 4 ignitions per year, wet LFM, and uniform ignition probabilities.

Figure 8. Fire Return Interval maps for 1000 years of fires for SMM, showing the effect of increasing the number of ignitions per year (igpy) from 1 to 12. Other parameters held constant were 4 Santa Ana events per year, wet LFM, and uniform ignition probabilities.

Figure 9. Fire Return Interval maps for 1000 years of fires for SMM, showing the effect of changing LFM from constant (a), to average dry trend (b), to average wet trend (c). Other parameters held constant were 4 Santa Ana events per year, 4 ignitions per year, and uniform ignition probabilities. Image (d) shows the effect of using correlated ignition probabilities where all other parameters are the same as (c).

Figure 10. Boxplots for number of ignitions per year, LFM trend, number of Santa Ana events per year, and spatial ignition pattern.

Figure 11. Contour plot of percentage area burned during Santa Ana events, generally showing more sensitivity to the number of Santa Anas as opposed to the number of ignitions.

Figure 12. Boxplots for the interaction of LFM and number of Santa Ana events per year. X-axis refers to 0-16 Santa Anas and constant (c), dry (d), and wet (w) LFM. For 0 Santa Anas, the dry LFM trend burned a much larger area than the other trends. At higher numbers of Santa Anas, the weather dominates, and all three LFM trends produce similar total area burned.

Figure 13. Boxplots for the interaction of LFM and number of ignitions per year. X-axis refers to 0-12 ignitions and constant (c), dry (d), and wet (w) LFM. For 0 ignitions, the constant LFM trend burned a much smaller area than the other trends. At higher numbers of ignitions, the weather dominates, and all three LFM trends produce similar total area burned.

Figure 1

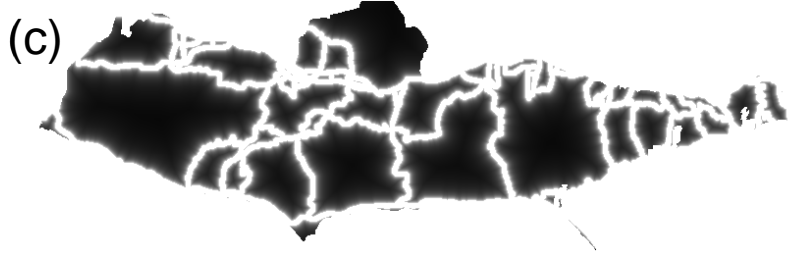
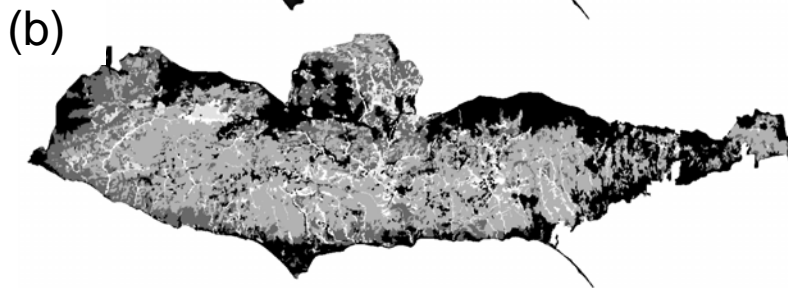
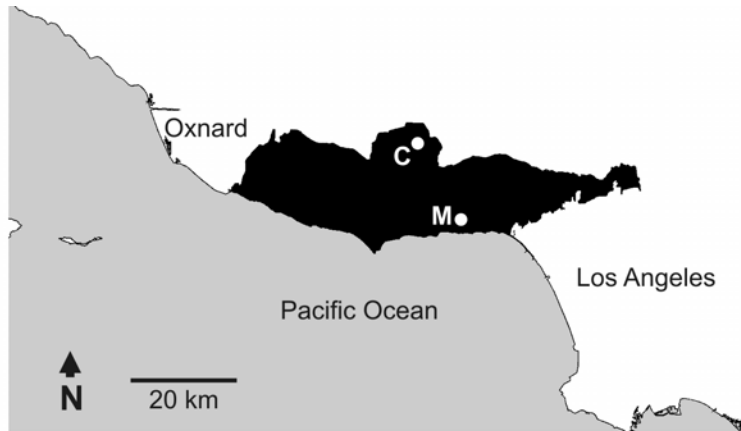


Figure 2

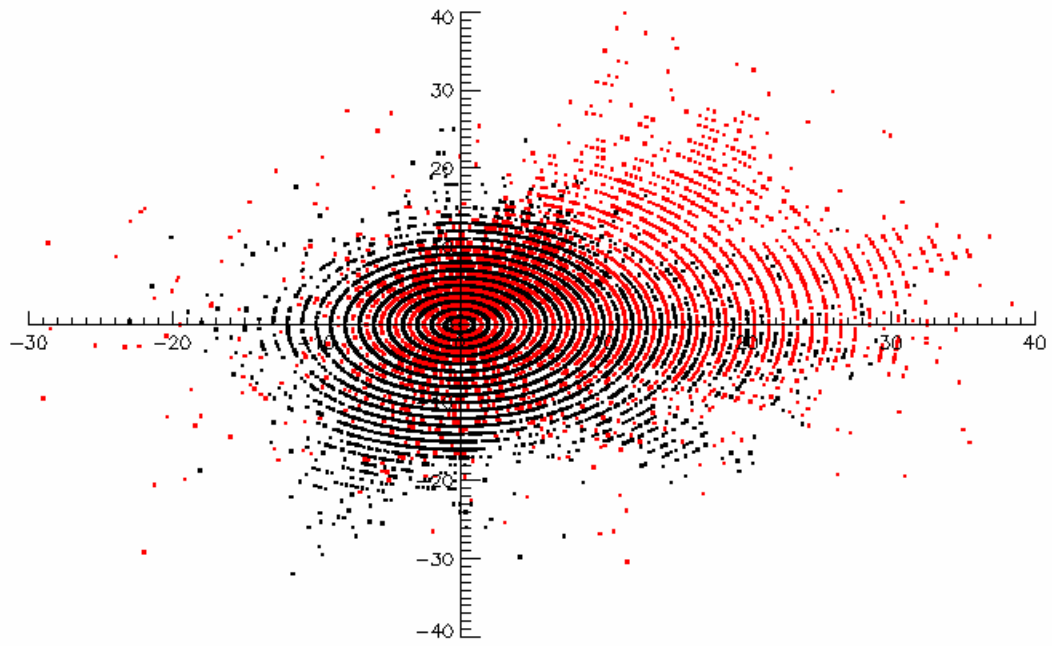


Figure 3

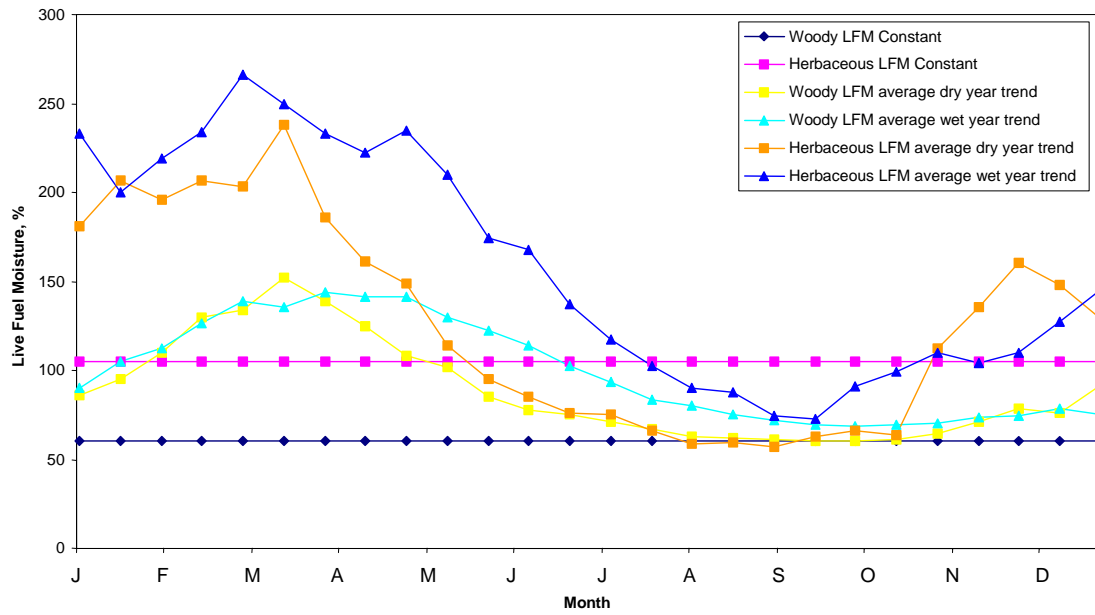


Figure 4

of
fires

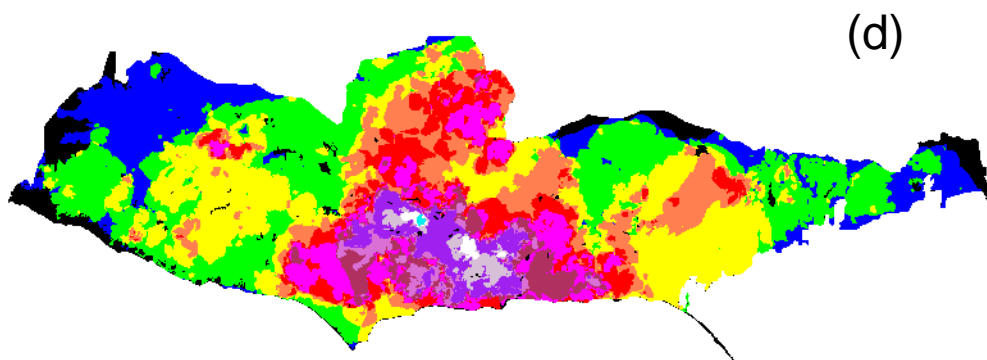
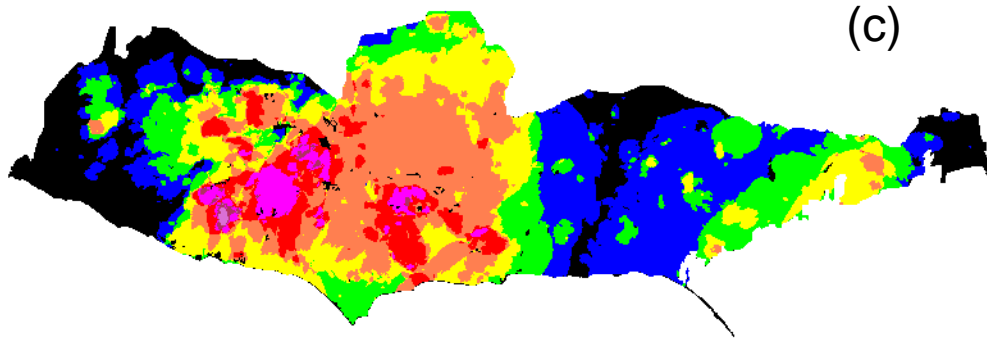
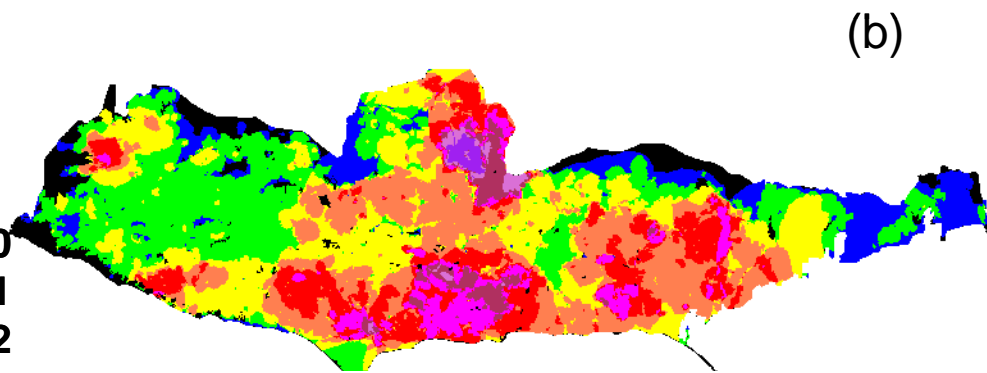
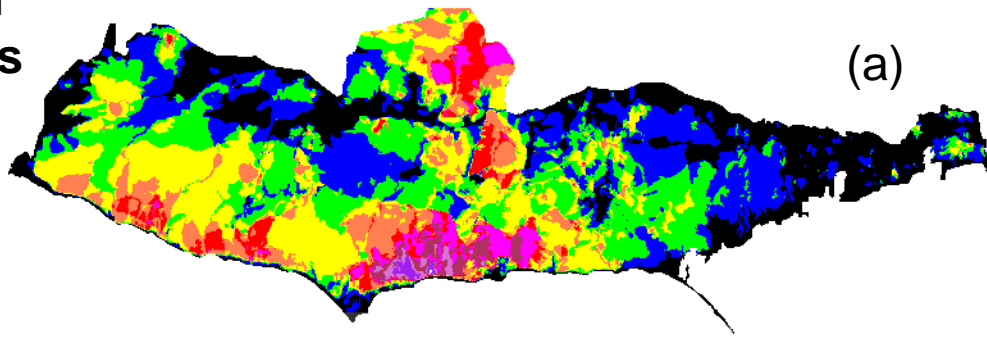
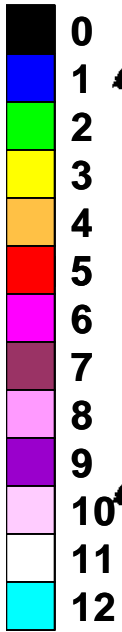


Figure 5

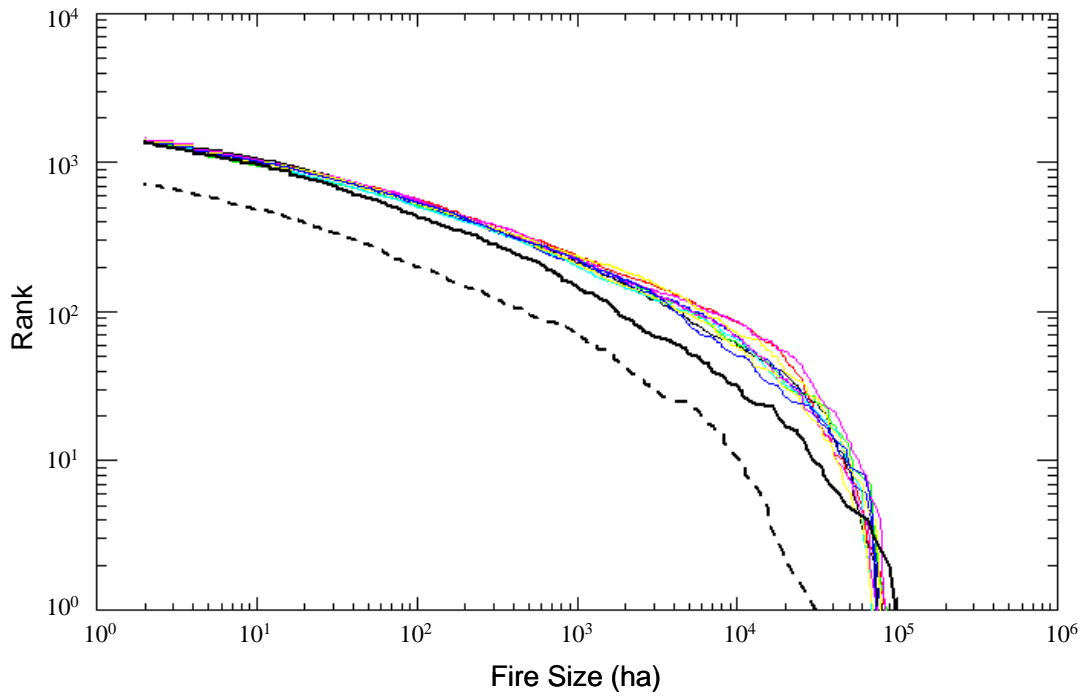


Figure 6

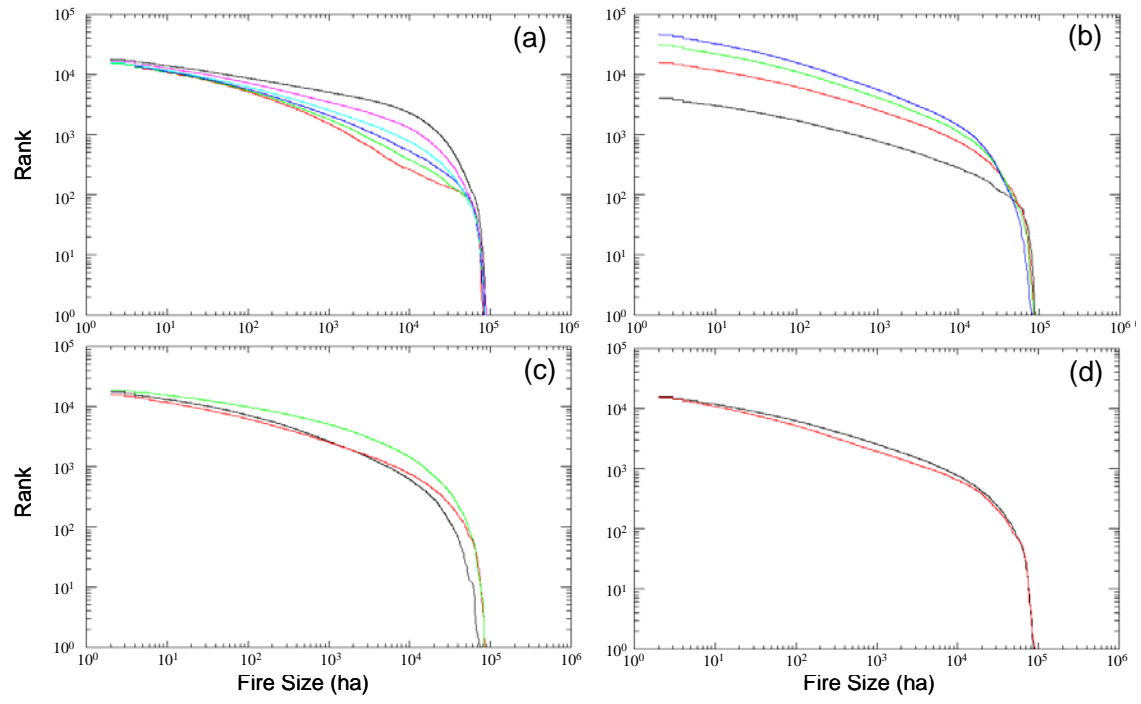
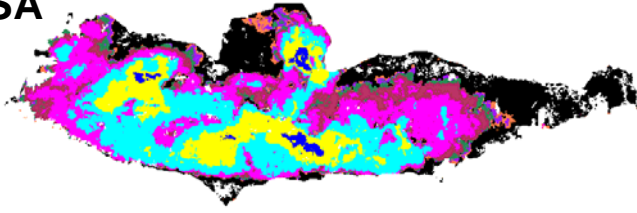
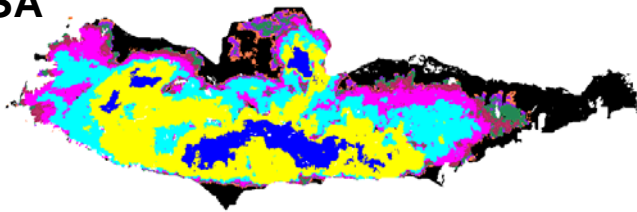


Figure 7

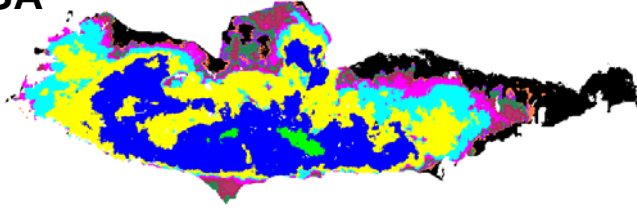
0 SA



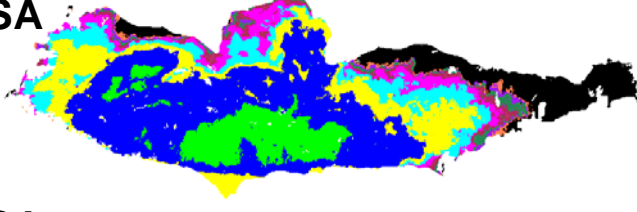
1 SA



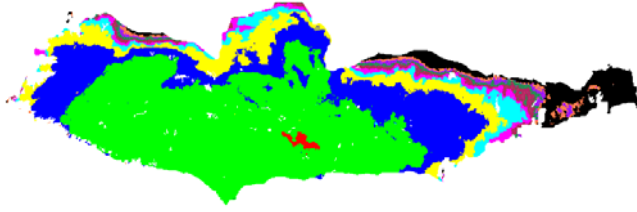
2 SA



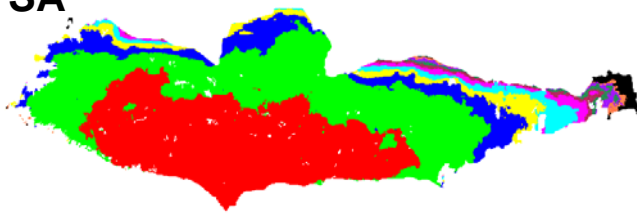
4 SA



8 SA



16 SA



FRI (years)

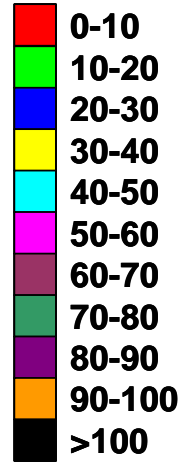
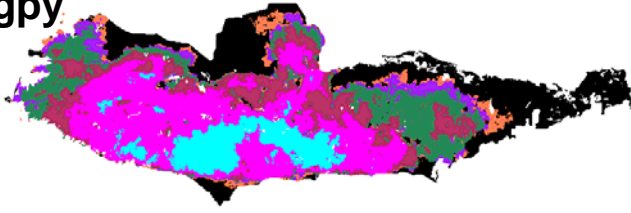
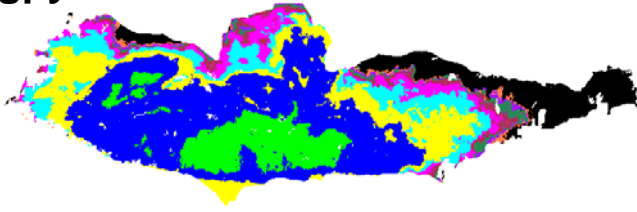


Figure 8

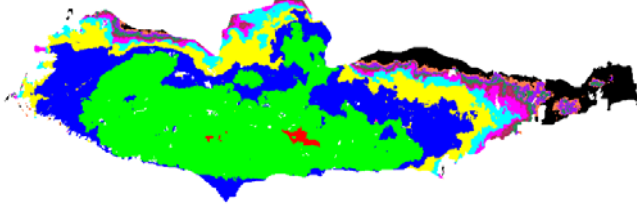
1 igpy



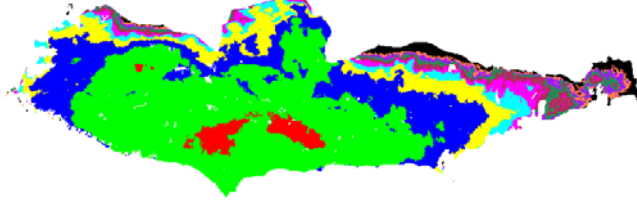
4 igpy



8 igpy



12 igpy



FRI (years)

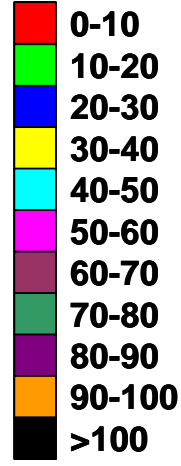
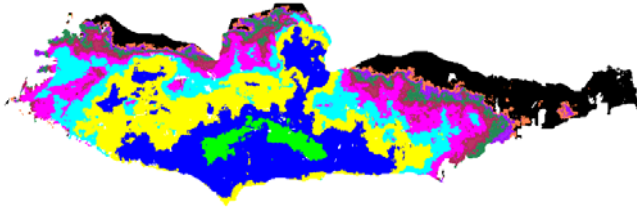
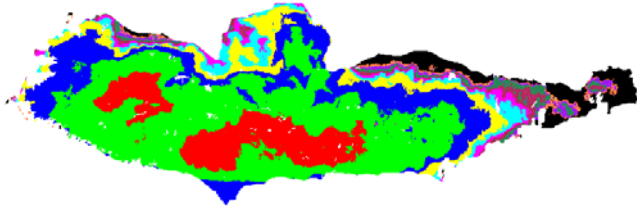


Figure 9

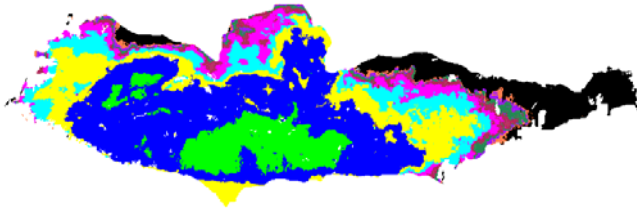
(a)



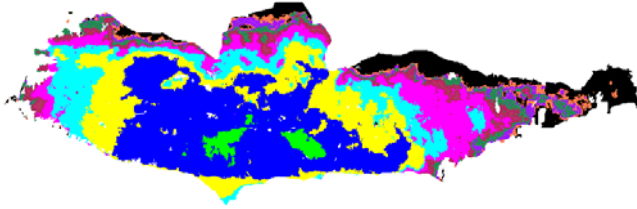
(b)



(c)



(d)



FRI (years)

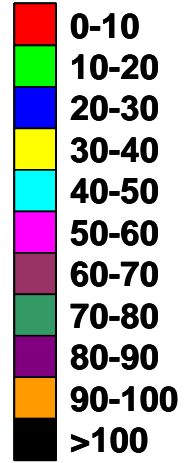


Figure 10

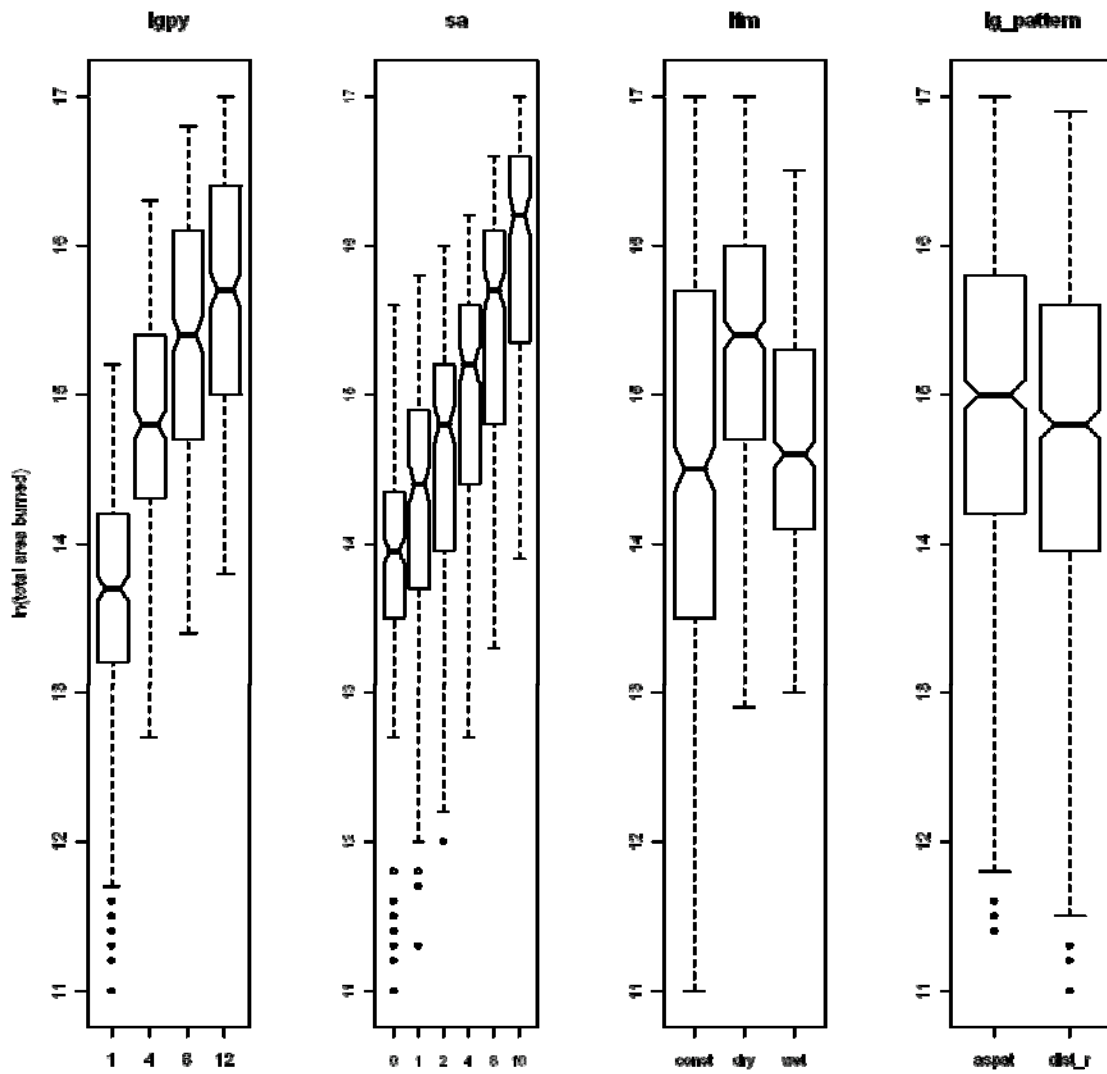


Figure 11

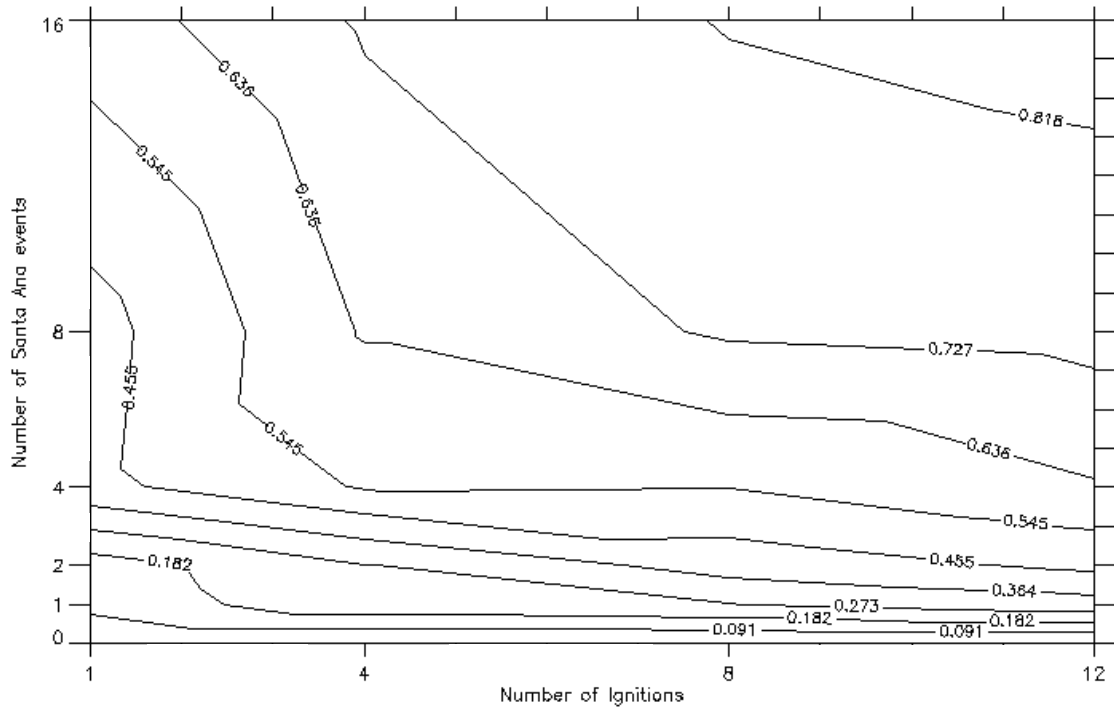


Figure 12

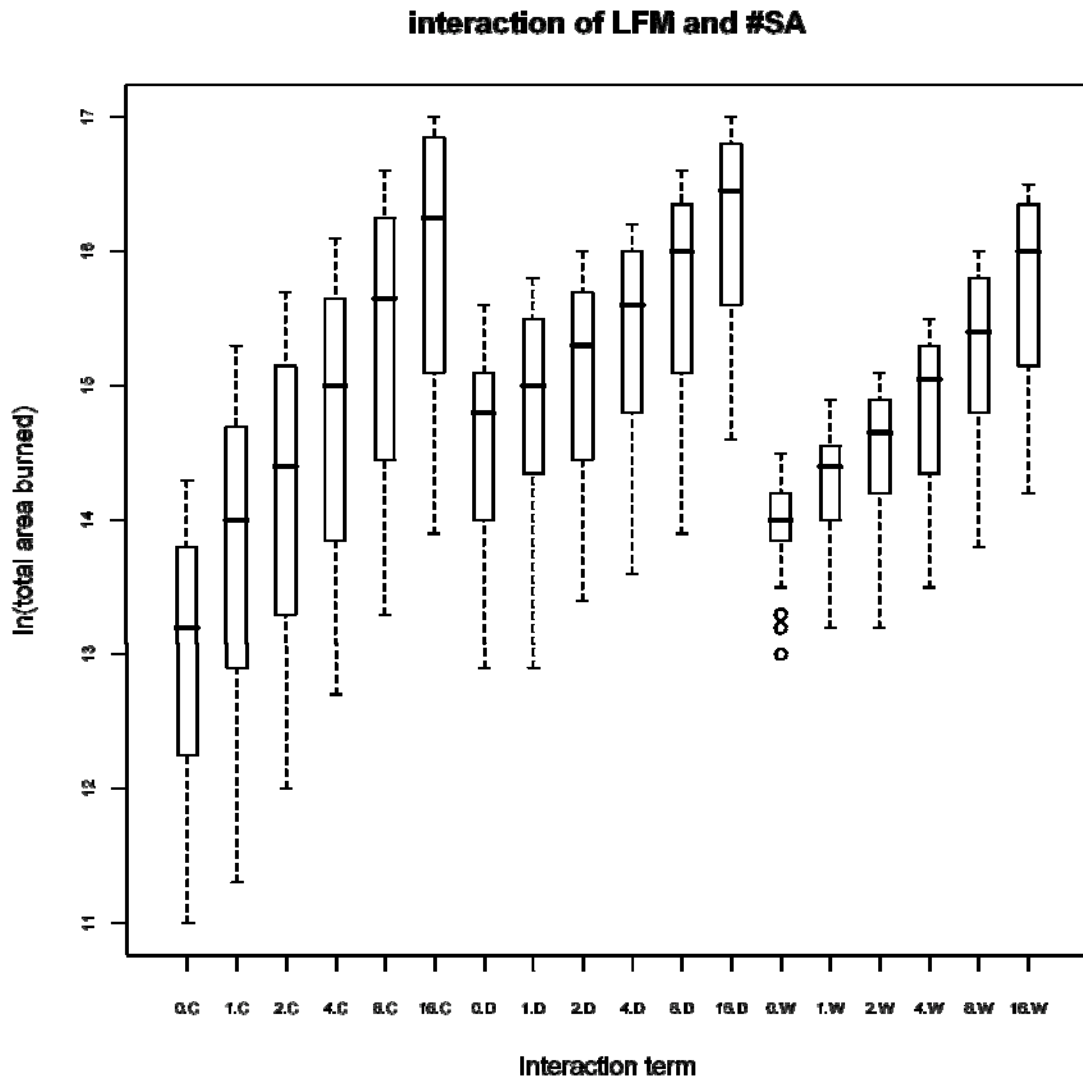
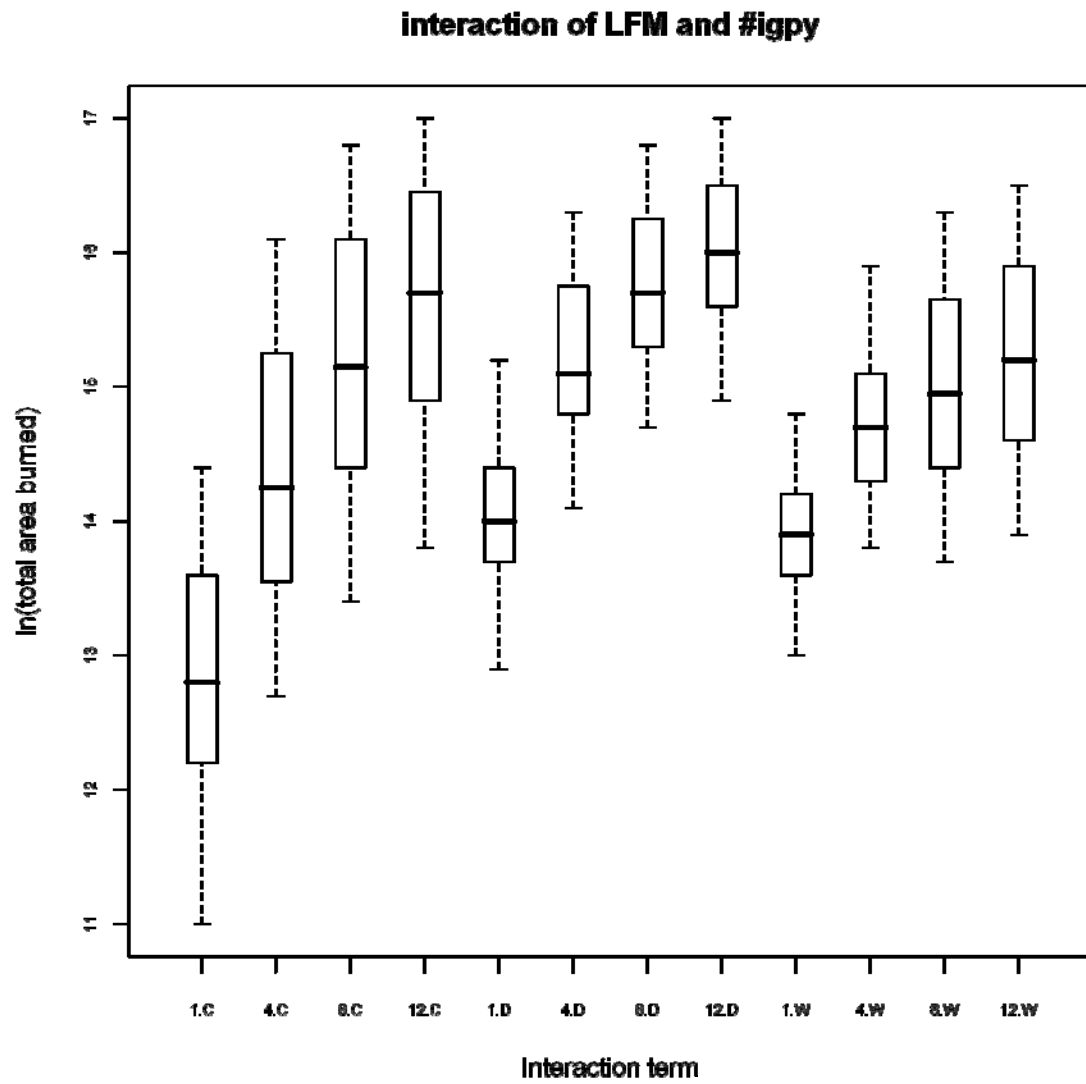


Figure 13



Online supporting materials: Appendix Table and Model Descriptions

Table A1. Standard Northern Forest Fire Laboratory (NFFL, Albini 1976) fuel model and custom fuel model (Weise and Regelbrugge 1997; Morais 2001) characteristics.

Fuel Model	Description	Dry Biomass of Dead Fuels (<0.635 cm) Mg/ha	Dry Biomass of Dead Fuels (0.635-2.54 cm) Mg/ha	Dry Biomass of Dead Fuels (2.54-7.62 cm) Mg/ha	Dry Biomass of Live Herb. Fuels Mg/ha	Dry Biomass of Live Woody Fuels Mg/ha	Surface Area-to-Volume Ratio of <0.635 cm Dead Fuels (1/cm)	Surface Area-to-Volume Ratio of Live Herb. Fuels (1/cm)	Fuel Bed Depth (cm)	Dead Fuel Moisture of Extinction (%)	Dead Fuel Heat Content (J/kg)	Live Fuel Heat Content (J/kg)
NFFL 1	short grass	1.66	0	0	0	0	105.98	0	30.48	12	18608	18608
NFFL 3	tall grass	6.75	0	0	0	0	45.42	0	76.20	25	18608	18608
NFFL 5	brush	2.24	1.12	0	0	4.48	60.56	0	60.96	20	18608	18608
NFFL 9	hardwood litter	6.55	0.92	0.34	0	0	75.7	0	6.10	25	18608	18608
Custom 15	old chamise	4.48	6.73	2.24	1.12	4.48	19.37	66.61	91.44	13	23260	23260
Custom 16	ceanothus	5.04	10.76	4.04	6.73	6.28	15.14	45.42	182.88	15	18608	18608
Custom 17	young chamise	2.91	2.24	2.24	4.48	4.48	19.37	66.61	121.92	20	18608	18608
Custom 18	sagebrush and buckwheat	12.33	1.79	0.22	1.68	5.6	19.37	45.42	91.44	25	21399	21399
Custom 20	WUI	1.66	4.19	3.36	0	0.83	105.98	45.42	53.34	40	18608	18608
Custom 21	SMM CSS	5.5	0.7	0	1.6	3	19.37	45.42	91.44	25	21399	21399

Model Name: "Short Grass"

Fuel Model Number: 1

Source: Albini 1976

Description:

This model corresponds to stands where the Potential Natural Vegetation (PNV) and cover was identified from Franklin, 1997 as consisting of:

- dominated by exotic annual grasses
- Valley Oak (*Quercus lobata*) savanna
- open Walnut (*Juglans californica*) woodlands
- coastal cactus scrub consisting of Prickly Pear (*Opuntia oricola*) and exotic annual grasses

Model Name: "Tall Grass"

Fuel Model Number: 3

Source: Albini 1976

Description:

This model corresponds to stands where the Potential Natural Vegetation (PNV) was identified from Franklin, 1997 as consisting of:

- Coast Live Oak (*Quercus agrifolia*) woodland

Model Name: "Brush"

Fuel Model Number: 5

Source: Albini 1976

Description:

This model corresponds to stands where the Potential Natural Vegetation (PNV) and cover was identified from Franklin, 1997 as consisting of:

- dominated by northern mixed chaparral AND less than or equal to 2 years maturity
- > 80% cover of Chamise (*Adenostoma fasciculatum*) AND less than or equal to 2 years maturity
- dominated by Redshank (*Adenostoma sparsifolium*) chaparral AND less than or equal to 2 years maturity
- dominated by coastal sage scrub AND less than or equal to 3 years maturity
- dominated by a mixed coastal sage scrub and northern mixed chaparral community AND less than or equal to 2 years maturity

Model Name: "Hardwood Litter"

Fuel Model Number: 9

Source: Albini 1976

Description:

This model corresponds to riparian areas identified from a 1997 National Park Service field-based inventory as well as the following subclasses in Franklin, 1997:

- riparian corridors
- non-native conifers and hardwoods

Model Name: "Old Chamise"

Fuel Model Number: 15

Source: Weise and Regelbrugge 1997

Description:

This model corresponds to stands where the Potential Natural Vegetation (PNV) was identified from Franklin, 1997 as consisting of:

- > 80% cover of Chamise (*Adenostoma fasciculatum*) AND greater than 15 years maturity
- dominated by Redshank (*Adenostoma sparsifolium*) chaparral AND greater than 15 years maturity

Model Name: "Ceanothus"

Fuel Model Number: 16

Source: Weise and Regelbrugge 1997

Description:

This model corresponds to stands where the Potential Natural Vegetation (PNV) was identified from Franklin, 1997 as consisting of:

- dominated by northern mixed chaparral AND greater than 12 years maturity
- dominated by a mixed coastal sage scrub and northern mixed chaparral community AND greater than 12 years maturity

Model Name: "Young Chamise"

Fuel Model Number: 17

Source: Weise and Regelbrugge 1997

Description:

This model corresponds to stands where the Potential Natural Vegetation (PNV) was identified from Franklin, 1997 as consisting of:

- > 80% cover of Chamise (*Adenostoma fasciculatum*) AND greater than or equal to 3 years maturity AND less than or equal to 15 years maturity
- dominated by Redshank (*Adenostoma sparsifolium*) chaparral AND greater than or equal to 3 years maturity AND less than or equal to 15 years maturity

Model Name: "Sagebrush and Buckwheat"

Fuel Model Number: 18

Source: Weise and Regelbrugge 1997

Description:

This model corresponds to stands where the Potential Natural Vegetation (PNV) was identified from Franklin, 1997 as consisting of:

- dominated by coastal sage scrub AND greater than 15 years maturity
- dominated by northern mixed chaparral AND greater than or equal to 3 years maturity AND less than or equal to 12 years maturity

Model Name: "Wildland Urban Interface"

Fuel Model Number: 20

Source: Morais 2001

Description:

This model corresponds to stands where the cover was identified from Franklin, 1997 as consisting of:

- rural residential or urban land use

This fuel model is meant to mimic the exotic landscape vegetation commonly surrounding homes in the Santa Monica Mountains. The grass component of the wildland urban interface fuels is represented by values of D1H and DSAV taken from NFFL 1. The exotic landscaped vegetation component of the wildland urban interface fuels is represented by values of D10H, D100H, LH, LW, LHS AV, and LWS AV taken from NFFL 7. The fuel bed depth is the numerical average of NFFL 1 and NFFL 7.

Model Name: "Santa Monica Mountains Coastal Sage Scrub"

Fuel Model Number: 21

Source: Morais 2001

Description:

This model corresponds to stands where the Potential Natural Vegetation (PNV) was identified from Franklin, 1997 as consisting of:

- dominated by coastal sage scrub AND greater than 3 years maturity AND less than or equal to 15 years maturity
- dominated by a mixed coastal sage scrub and northern mixed chaparral community AND less than or equal to 12 years maturity

Fuel biomass data collected from destructive sampling of coastal sage scrub sites in the Santa Monica Mountains displayed much lower loading values as compared to model 18 developed by the US Forest Service. The values used for fuel biomass in this fuel model represent values closer to what was recorded from the destructive samples taken in the Santa Monica Mountains.